

Search for Hybrid Baryons with CLAS12 experimental setup ECT* workshop

Lucilla Lanza, Ph. D. student

Supervisor: prof. Annalisa D'Angelo

University of Rome, Tor Vergata

INFN

13 October 2015



Outline

Physics motivation: Search of Hybrid Baryons contributions in the low Q^2 evolution of the cross section for $K^+\Lambda$ electro-production in CLAS12
→ Endorsement of a Letter of Intent by the Program Advisory Committee, PAC43. In this Lol the role of the Forward Tagger (FT) experimental setup is crucial to cover the very low Q^2 kinematical regions.

- **FT Software:** Optimization the FT-Cal cluster reconstruction algorithm and the calibration procedure using the π^0 decay into two photons, and single photon events.
- **Simulation and fast mc reconstruction** of $K^+\Lambda$ electro-production events in CLAS12

Hybrid Baryons

Hybrid Baryons: baryons with explicit gluonic degrees of freedom

Augmenting the quarks q by gluons g leads to **additional states** in the spectrum relative to the expectations of the naive quark model. Physically allowed (color singlets) states in the baryon spectrum may be constructed from $|qqqg\rangle$ «hybrid» basis states, in addition to the familiar $|qqq\rangle$ quark model states:

$$|qqq\rangle|_{\text{color}} = 1 \otimes 8 \otimes 8 \otimes 10,$$

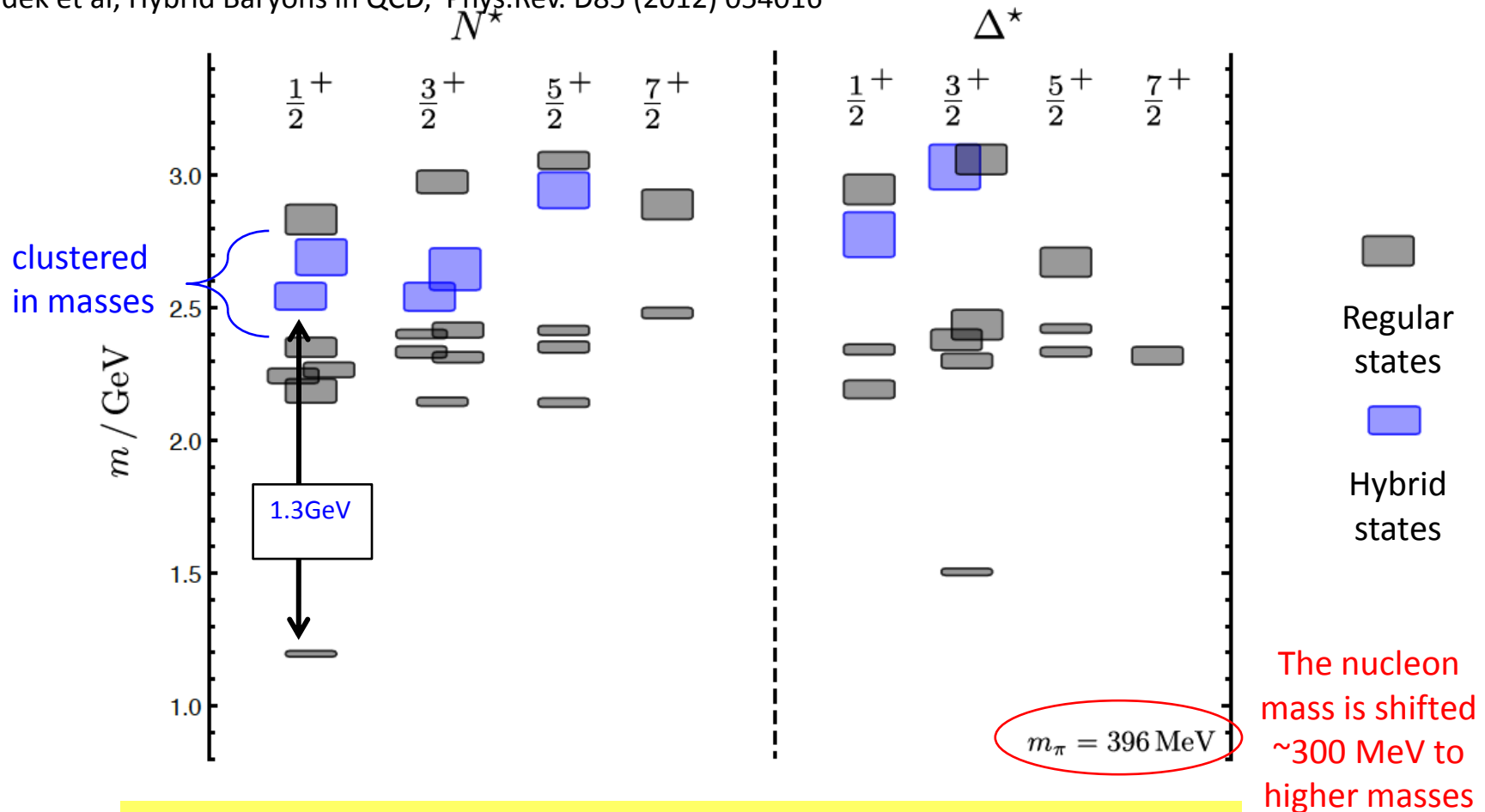
$$|qqqg\rangle|_{\text{color}} = (1 \otimes 8 \otimes 8 \otimes 10) \otimes 8$$

Hybrid Baryons in LQCD

QCD allows for the existence of Hybrid Baryons.

LQCD predicts several hybrid baryons states.

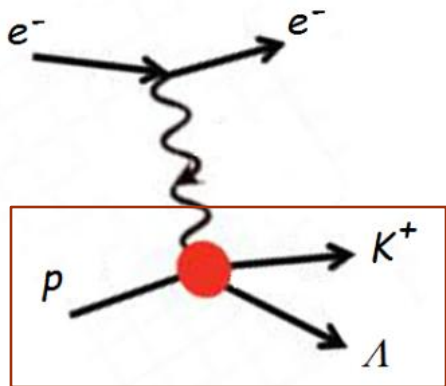
J. Dudek et al, Hybrid Baryons in QCD, Phys.Rev. D85 (2012) 054016



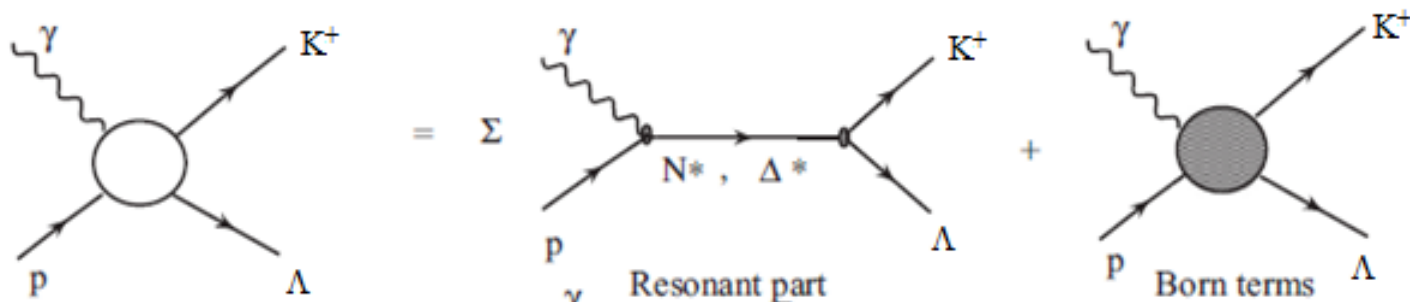
Differently from the case of hybrid mesons, hybrid baryons are predicted to have **same quantum numbers** of N^* resonances

Separating Q^3G from Q^3 states: $A_{1/2, 3/2}(Q^2)$ and $S_{1/2}(Q^2)$

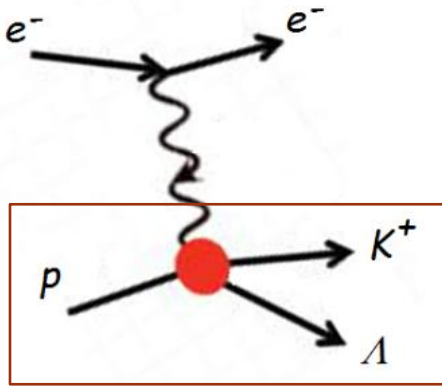
Transverse elicity amplitude $A_{1/2}(Q^2)$, $A_{3/2}(Q^2)$ and longitudinal elicity amplitude $S_{1/2}(Q^2)$ allow to distinguish Q^3G from Q^3 states



Electroexcitation via quasi-real photon exchange can be considered for practical purposes photo-production



Separating $Q^3 G$ from Q^3 states: $A_{1/2, 3/2}(Q^2)$ and $S_{1/2}(Q^2)$



Resonant contribution in the helicity representation

$$\langle \lambda_f | T_r | \lambda_\gamma \lambda_p \rangle = \sum_{N^*} \frac{\langle \lambda_f | T_{dec} | \lambda_R \rangle \langle \lambda_R | T_{em} | \lambda_\gamma \lambda_p \rangle}{M_r^2 - W^2 - i\Gamma_r(W)M_r}$$

Helicities of final state hadrons λ_f and λ_p and λ_γ and λ_p

N^* helicity = $\lambda_\gamma - \lambda_p$

where

M_r : Resonance mass
 W : Invariant mass
 $\Gamma_r(W)$: Energy dependent total width

The N^* hadronic decay amplitudes can be expanded in **partial waves** of total momentum J

$$\langle \lambda_f | T_{dec} | \lambda_R \rangle = \langle \lambda_f | T_{dec}^{J_r} | \lambda_R \rangle d_{\mu\nu}^{J_r}(\cos \theta^*) e^{i\mu\phi^*} \quad \text{where} \quad \langle \lambda_f | T_{dec}^{J_r} | \lambda_R \rangle = \frac{2\sqrt{2\pi} \sqrt{2J_r + 1} M_r \sqrt{\Gamma_{\lambda_f}}}{\sqrt{\langle p_i' \rangle}} \sqrt{\langle p_i \rangle}$$

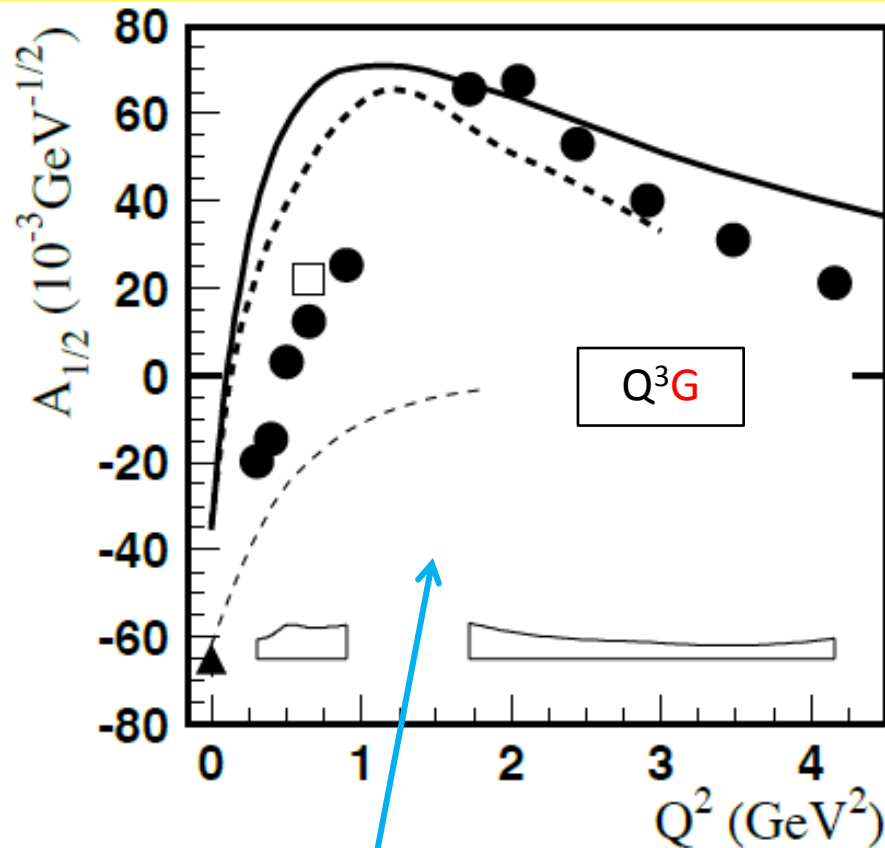
The **resonance electroexcitation amplitudes** can be related to the $\gamma_\nu NN^*$ electrocouplings $A_{1/2}, A_{3/2}$, and $S_{1/2}$ for nucleons

$$\langle \lambda_R | T_{em} | \lambda_\gamma \lambda_p \rangle = \frac{W}{M_r} \sqrt{\frac{8M_N M_r q_{\gamma r}}{4\pi\alpha}} \sqrt{\frac{q_{\gamma r}}{q_\gamma}} A_{1/2, 3/2}(Q^2) \quad \text{with} \quad |\lambda_\gamma - \lambda_p| = \frac{1}{2}, \frac{3}{2} \quad \text{for transverse photons,}$$

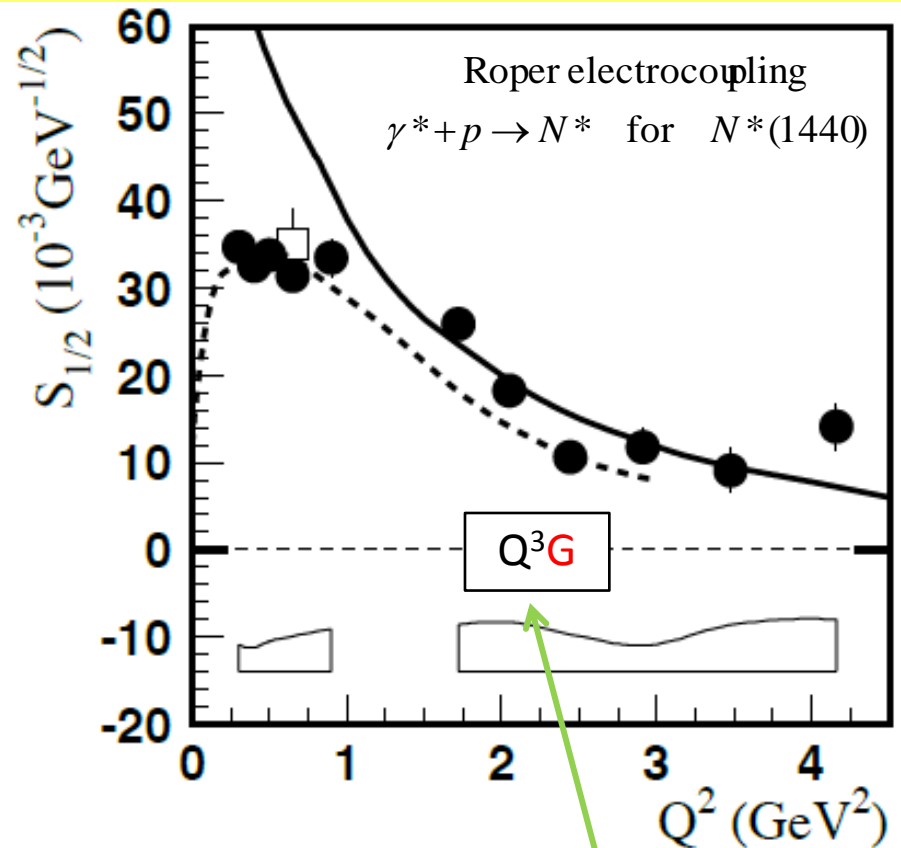
$$\langle \lambda_R | T_{em} | \lambda_\gamma \lambda_p \rangle = \frac{W}{M_r} \sqrt{\frac{16M_N M_r q_{\gamma r}}{4\pi\alpha}} \sqrt{\frac{q_{\gamma r}}{q_\gamma}} S_{1/2}(Q^2) \quad \text{for longitudinal photons}$$

Separating Q^3G from Q^3 states

Transverse helicity amplitude $A_{1/2}(Q^2)$ and longitudinal helicity amplitude $S_{1/2}(Q^2)$ allow to distinguish Q^3G from Q^3 states



A drop of the transverse helicity amplitudes $A_{1/2}(Q^2)$ faster than for ordinary three quark states, because of extra glue-component in valence structure



A suppressed longitudinal amplitude $S_{1/2}(Q^2)$ in comparison with transverse electro-excitation amplitude

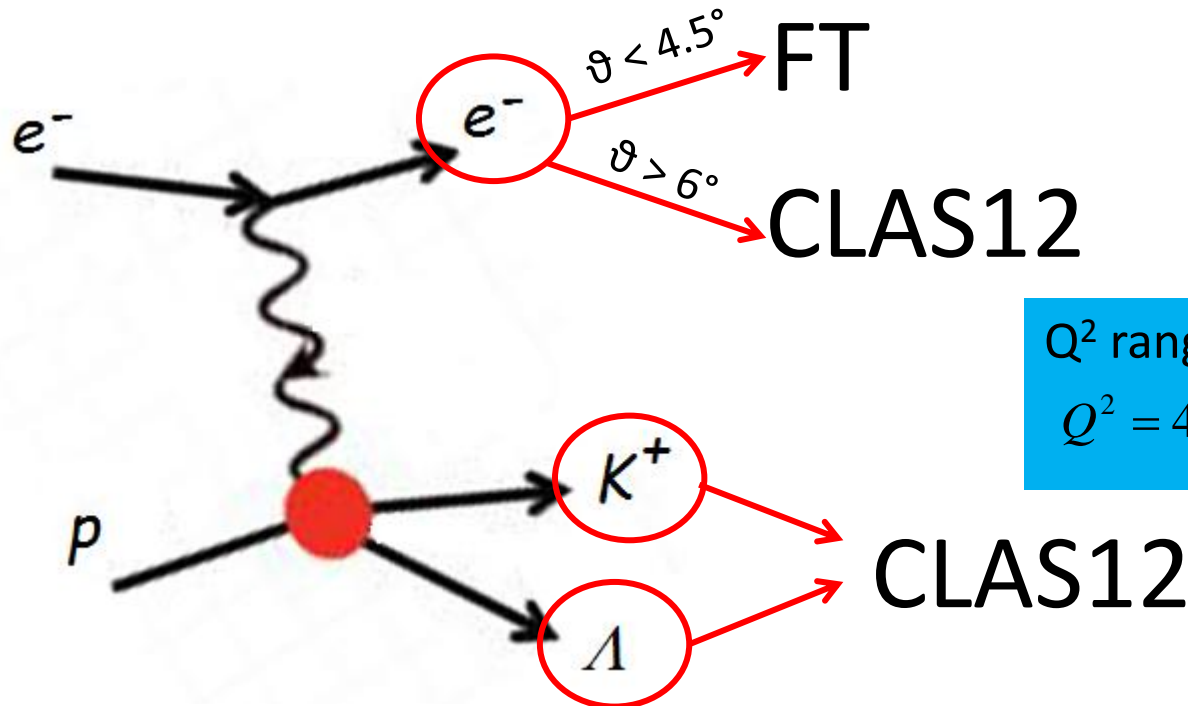
Signature

Based on available knowledge, the *signature* for hybrid baryons may consist of :

- Extra resonances with masses with $J^P=1/2^+$ from 1.8 GeV to 2.5 GeV and decays to $N\pi\pi$ or KY final states
- A drop of the transverse helicity amplitudes $A_{1/2}(Q^2)$ and $A_{3/2}(Q^2)$ faster than for ordinary three quark states, because of extra glue-component in valence structure
- A suppressed longitudinal amplitude $S_{1/2}(Q^2)$ in comparison with transverse electro-excitation amplitude

Experiment

Scattered electrons will be detected in Forward Tagger for angles from 2.5° to 4.5° . FT allows to probe the **crucial Q^2 range** where hybrid baryons may be identified due to their fast dropping $A_{1/2}(Q^2)$ amplitude and the suppression of the scalar $S_{1/2}(Q^2)$ amplitude.



Q^2 range of interest: $0.05 - 2 \text{ GeV}^2$
 $Q^2 = 4E_{\text{Beam}}E_e \sin^2 \frac{\vartheta}{2} \Rightarrow \vartheta < 5^\circ$

Scattered electrons will be detected in the Forward Detector of CLAS12 for scattering angles greater than about 6° . Charged hadrons will be measured in the full range from 6° to 130° .

The Forward Tagger (FT): Experimental Setup

FT-Cal

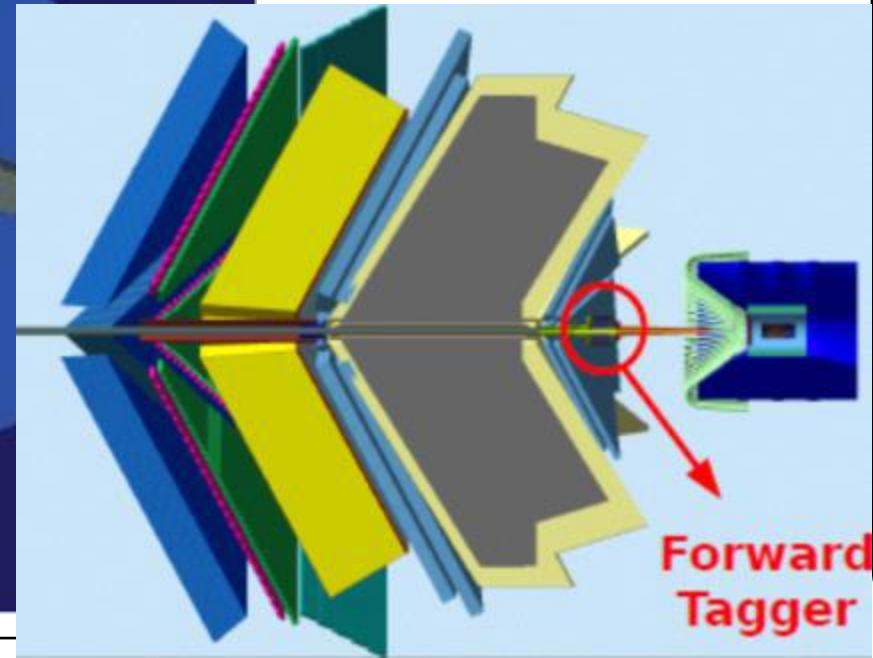
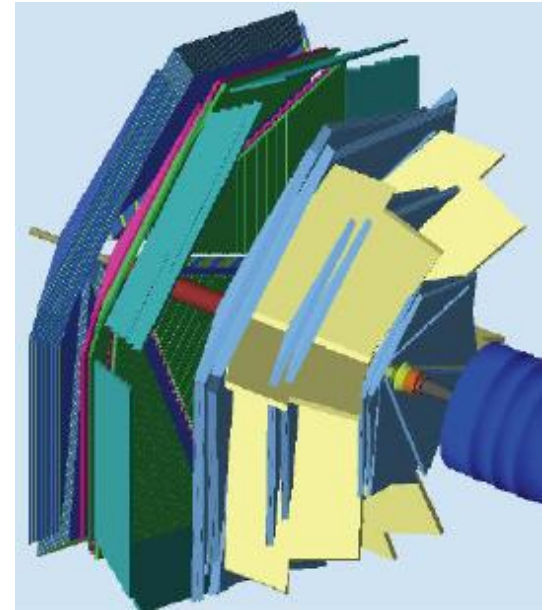
- Measurement of the EM shower Energy
- Fast trigger signal

FT-Trck

- Measurement of the scattering angles θ and ϕ

FT-Hodo

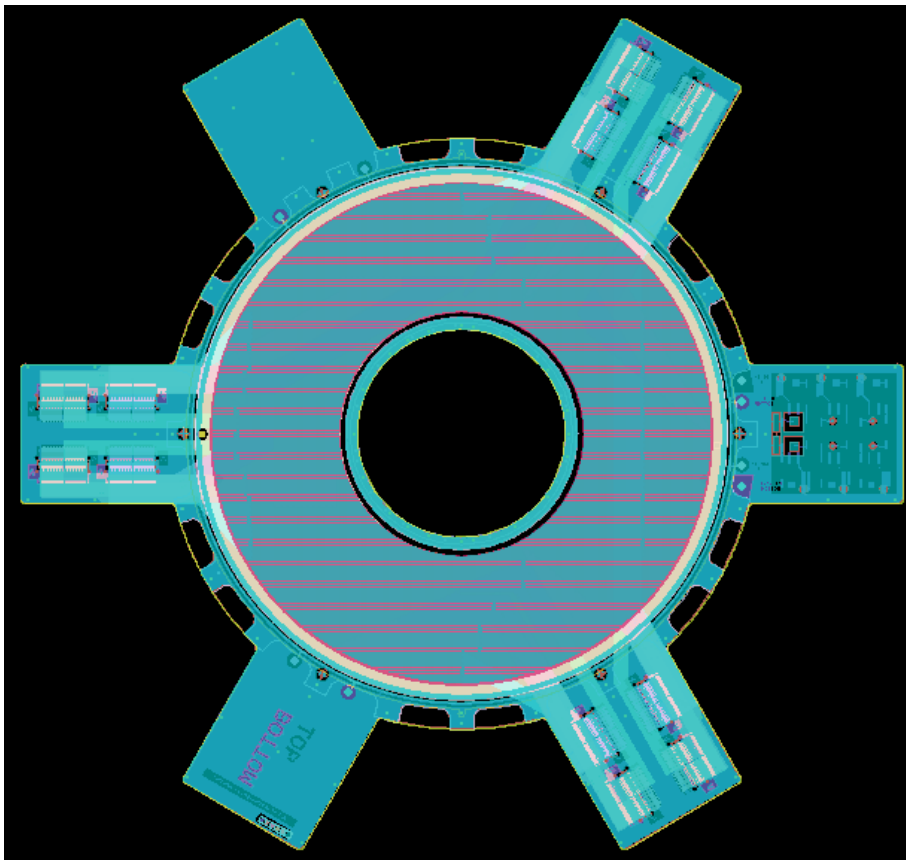
- Provides the e/ γ separation



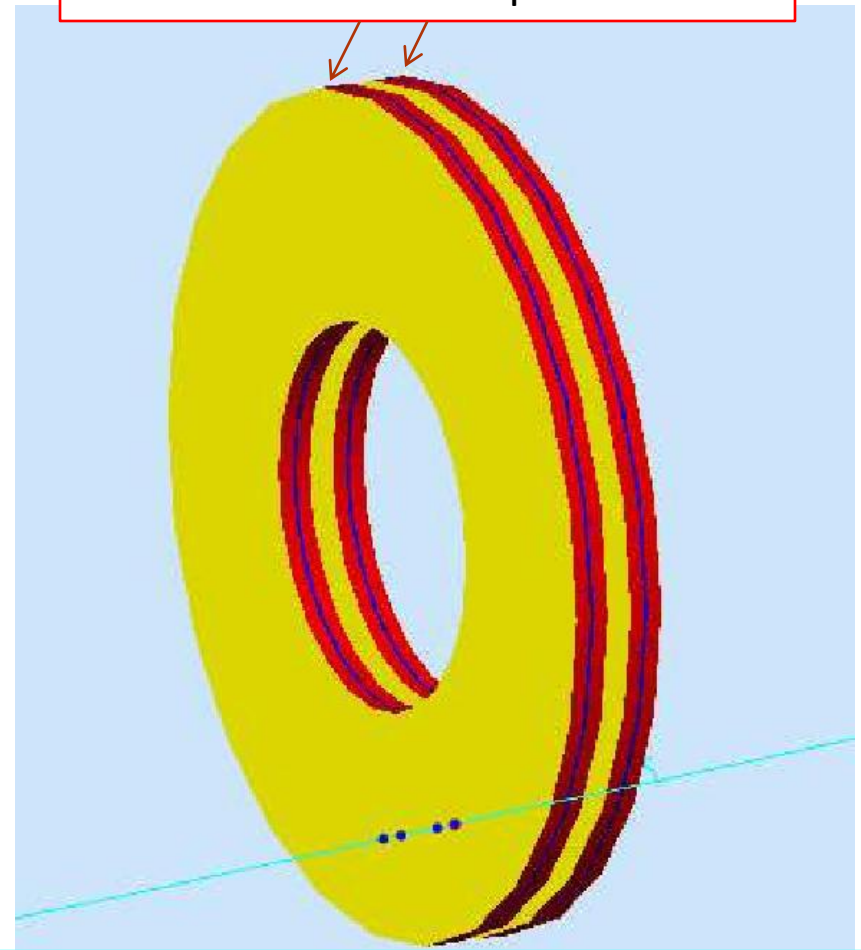
The Tracker (FT-Trck)

Micromegas detectors exploit the gas ionization process with charged particles to:

- Reconstruct the electron point of impact and path



Two layers of pairs of Micromegas detectors with strip readout

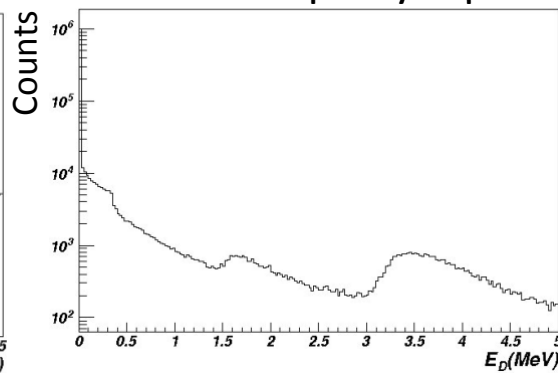
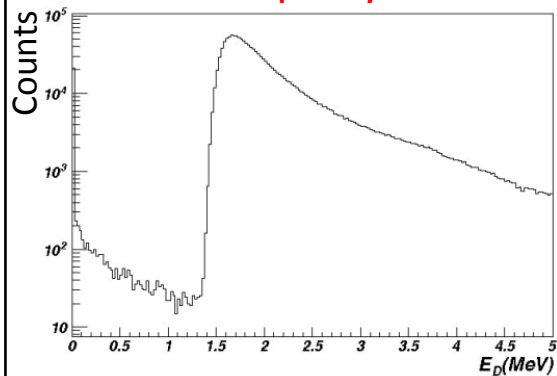


The strips of two different Micromegas in the same layer are orthogonal to produce a (x,y) couple

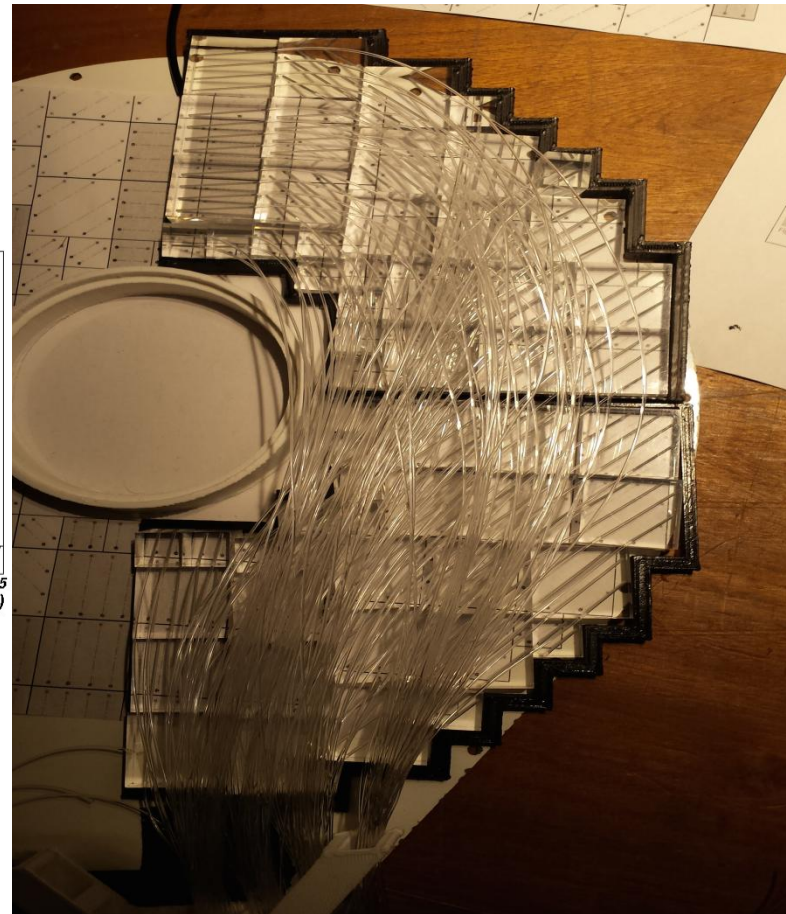
The Hodoscope (FT-Hodo)

E released in the
hodoscope by an e^-

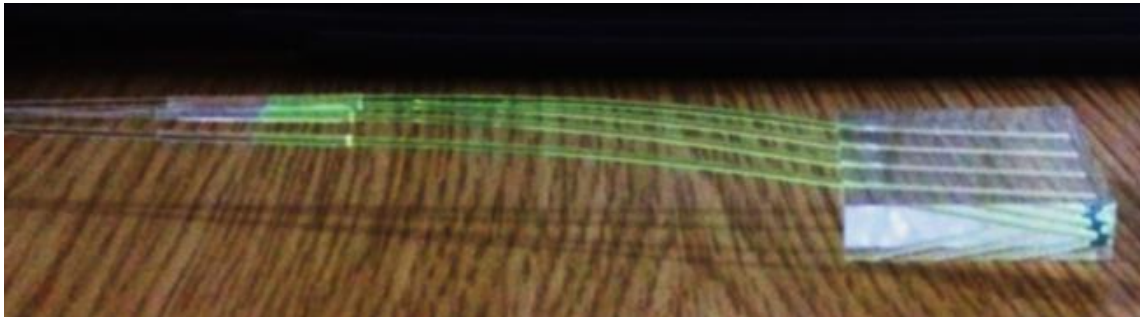
E released in the
hodoscope by a γ



232 scintillator tiles, 752 fibers in total



Wavelength shifting
(WLS)
fibres

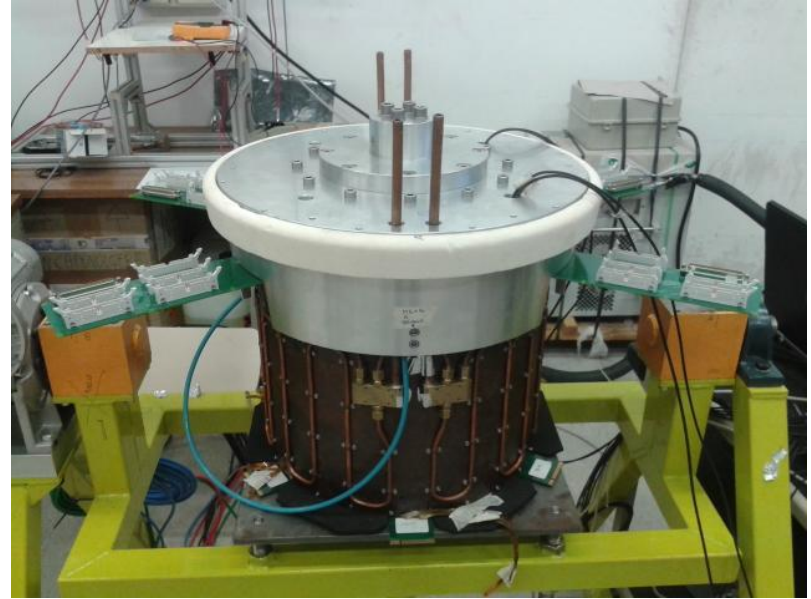


Two layers of
plastic
scintillator tiles

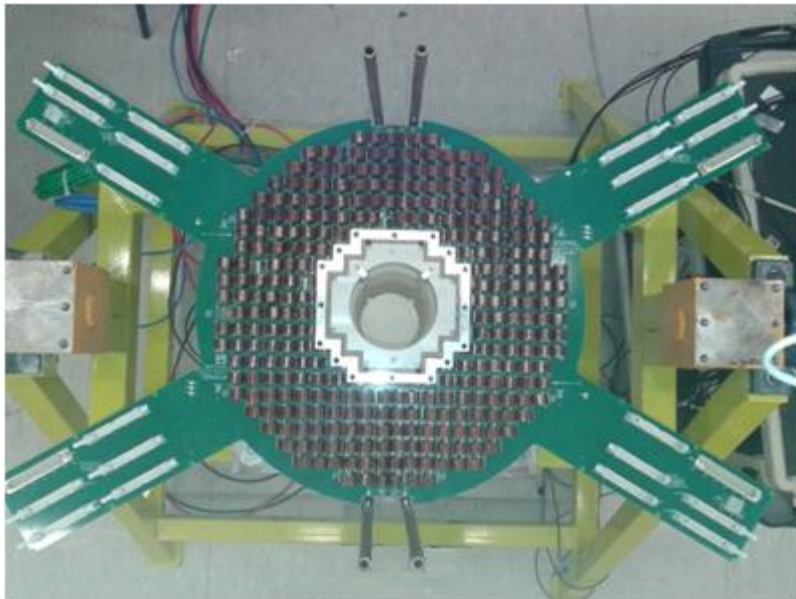
The Electromagnetic Calorimeter (FT-Cal)

Requirements:

- High radiation hardness
- High light yield
- Small radiation length and Moliere radius
- Fast recovery time
- Good energy and time resolution



Modules of PbWO_4 scintillating crystals



Pros

- High density (8.28 g/cm^3)
- Small radiation length (0.9 cm)
- Very fast decay time (6.5 ns)
- Very high radiation hardness

Contra

- Poor LY (fraction of % of the NaI one) (100-200 γ/MeV)
- Temperature must be controlled to avoid variations in gain and noise

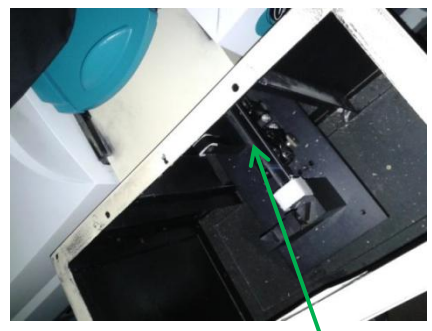
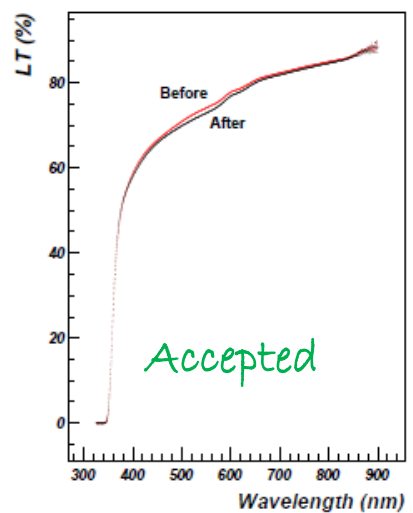
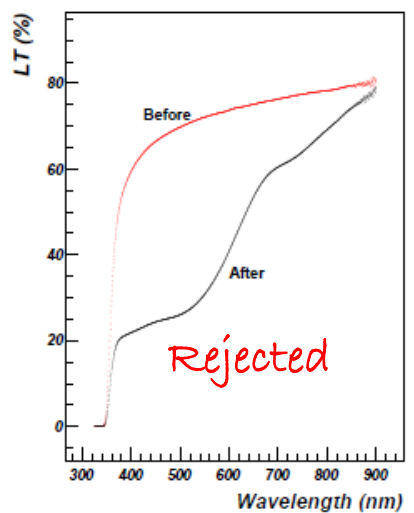
FT-Cal: PWO crystals

Modules of PbWO₄ scintillating crystals

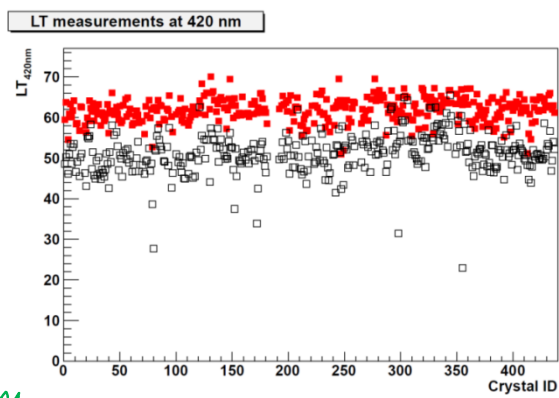


Pros	Contra
<ul style="list-style-type: none"> • High density (8.28 g/cm³) • Small radiation length (0.9 cm) • Very fast decay time (6.5 ns) • Very high radiation hardness 	<ul style="list-style-type: none"> • Poor LY (fraction of % of the NaI one) (100-200 γ/MeV) • Temperature must be controlled to avoid variations in gain and noise

Giessen measurements: employment of a **spectrophotometer** to perform hardness tests –LT before and after irradiation- on the **332 PWO crystals** that compose the FT calorimeter.



SICCAS 20 cm
PbWO₄



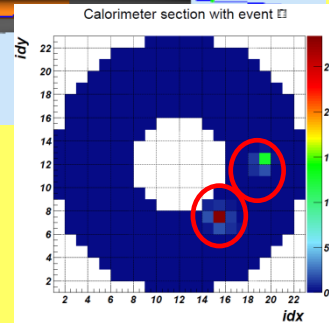
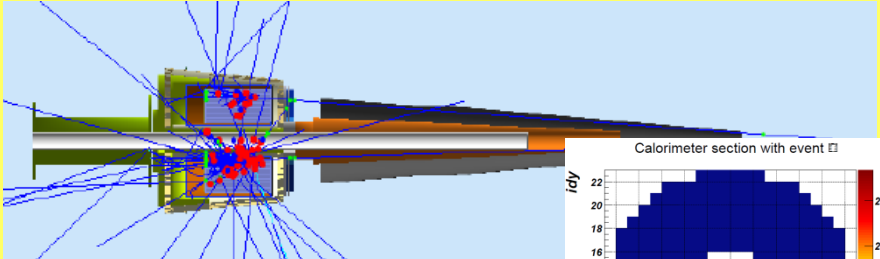
NIM paper:

Assessing the performance under ionising radiation of lead tungstate scintillators for EM calorimetry in the CLAS12 Forward Tagger

S. Fegan^{a,*}, E. Auffray^b, M. Battaglieri^a, E. Buchanan^c, B. Caiffi^a, A. Celentano^a, L. Colaneri^d, A. D'Angelo^d, R. De Vita^a, V. Dormenev^e, E. Fanchini^a, L. Lanza^d, R.W. Novotny^e, F. Parodi^a, A. Rizzo^d, D. Sokhan^c, I. Tarasov^f, I. Zonta^d

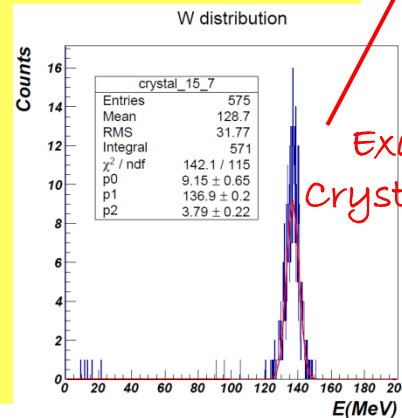
CLAS12 FT-Cal cluster reconstruction algorithm: Calibration using $\pi^0 \rightarrow \gamma\gamma$ process

- Generation of events with a $\pi^0 \rightarrow \gamma\gamma$ with GEMC (GEant4 MonteCarlo)



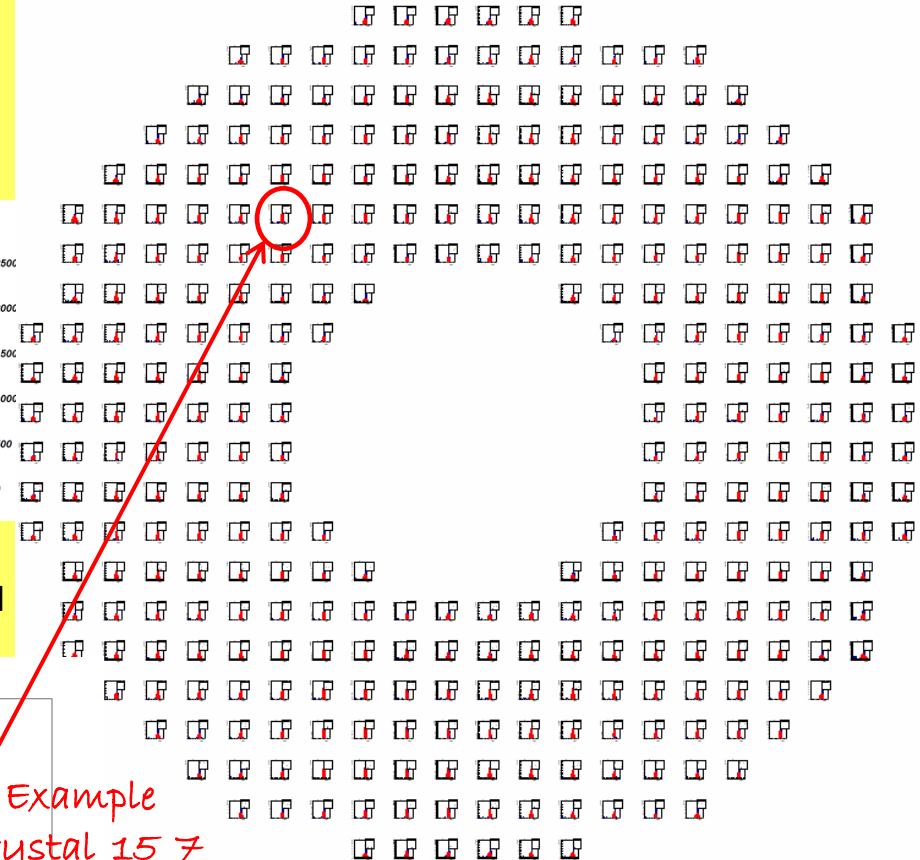
- Search for events with two photons using the flux detectors
- Identification of the clusters corresponding with the couple of photons:

- Only hits having a minimum energy are considered
- Reconstruction of the invariant mass of the two clusters: the invariant mass value is inserted in the histograms of the crystals that take part to the clusters
- Gaussian fit



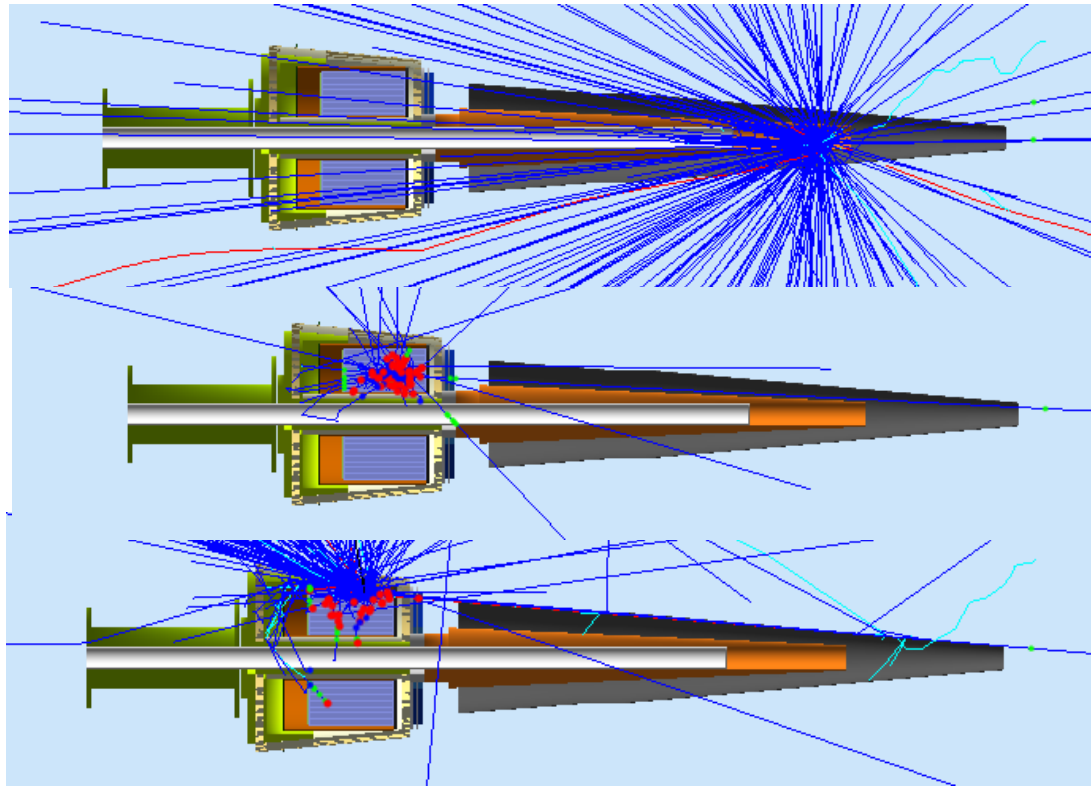
Example
Crystal_15_7

Distribution of the invariant mass of from each of the 332 PWO crystals



Hits: events in a single crystal whose amplitude is more than a threshold fixed at 10 MeV
Clusters: sets of hits corresponding to electromagnetic showers in the calorimeter.

Energy corrections as a function of ϑ and E using single photon events



$\vartheta = 2.15^\circ$

$\vartheta = 3.5^\circ$

$\vartheta = 4.85^\circ$

We expect a better reconstruction of cluster energy for intermediate values of ϑ ($2.5^\circ < \vartheta < 4.5^\circ$)

Simulation of single photon events have been performed using angles from 2.5° up to 4.5° , with steps of 0.2° and with photon energy $100 \text{ MeV} < E_{gen} < 8 \text{ GeV}$

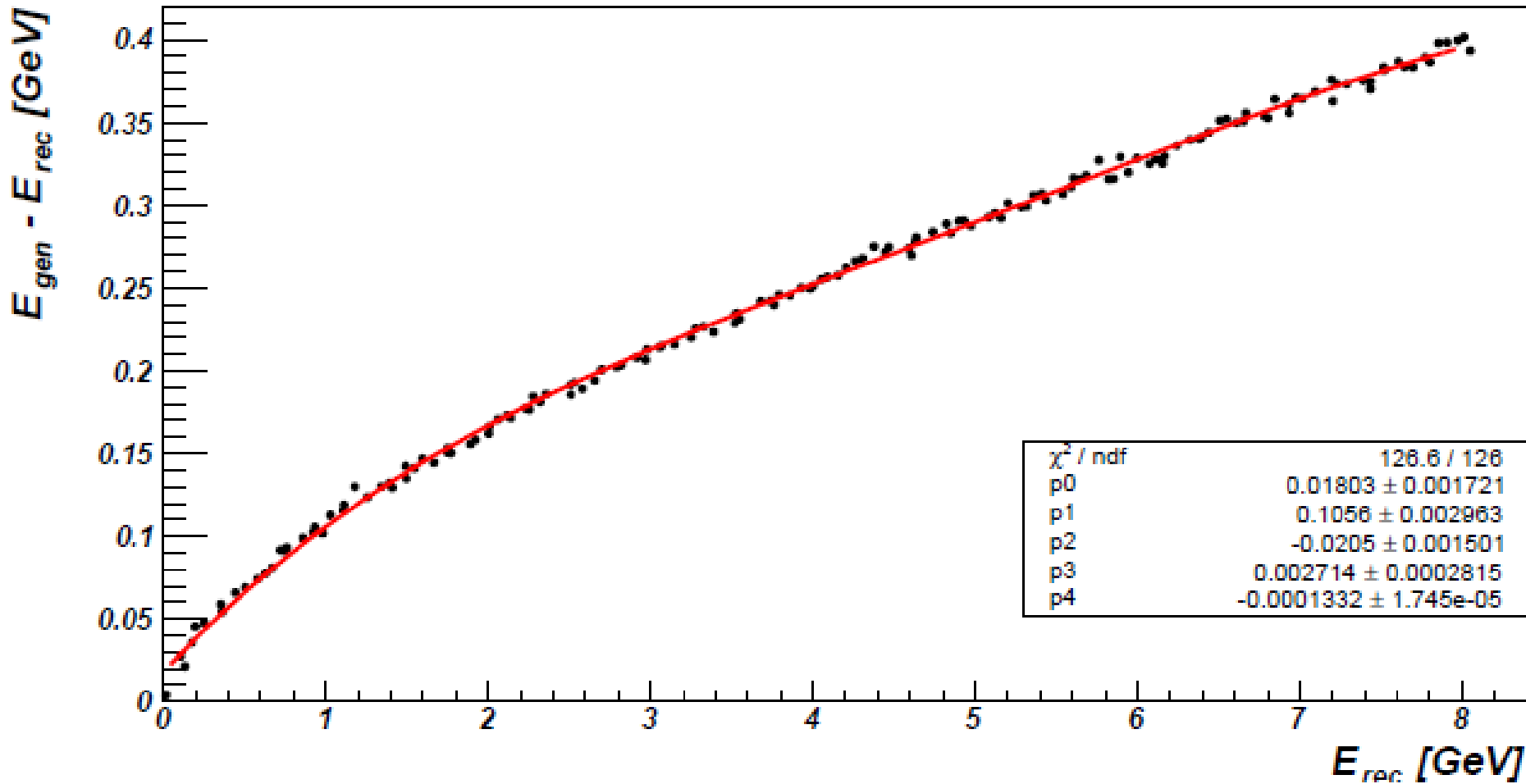
•Analysis procedure:

- Generation of events with GEMC
- Each event in the same .ev file is generated with random energy in the range $[0.1, 8] \text{ GeV}$, and with ϑ fixed at $2.5^\circ, 2.7^\circ, 2.9^\circ, \dots, 4.5^\circ$
- The algorithm reconstructs the energy for each event and divides events in energy bins on the basis of their energy
- For each bin the difference between the reconstructed and the generated energies is displayed.

16

- The distributions are fitted with gaussian functions whose means and sigmas are saved for the analysis
- The procedure is repeated for a new set of events characterized by a different ϑ

$E_{\text{gen}} - E_{\text{rec}}$ vs E_{rec} , $\vartheta = 3.5^\circ$



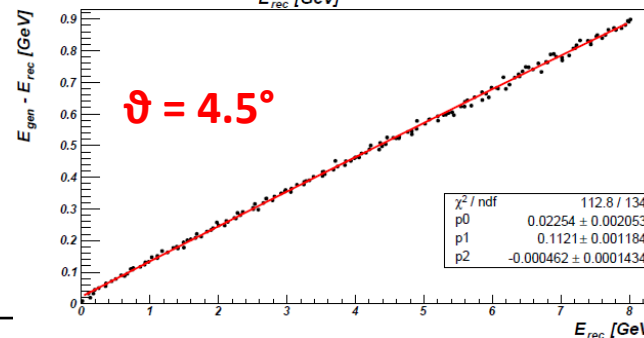
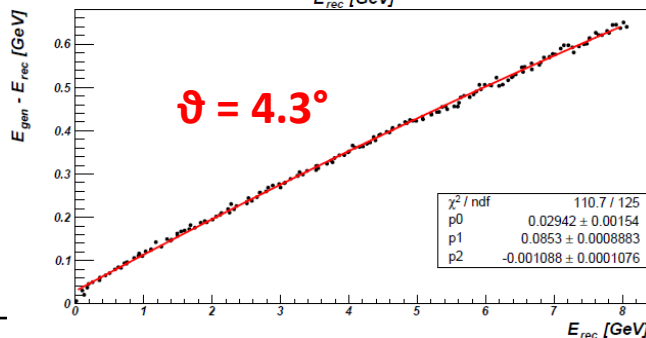
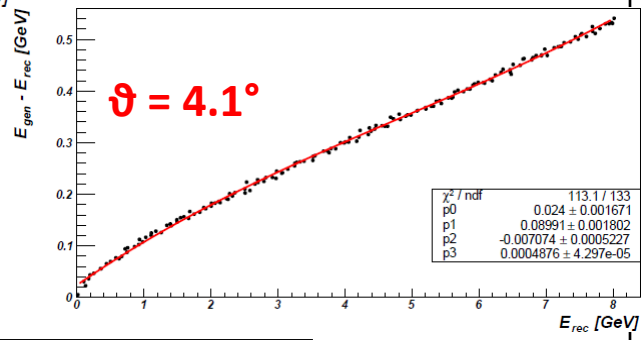
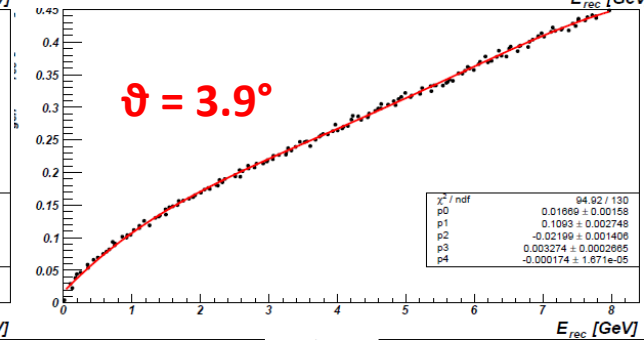
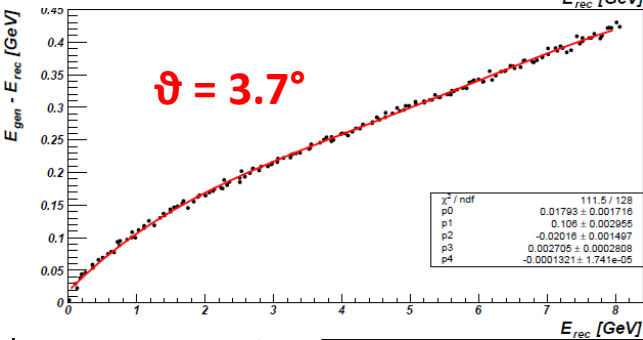
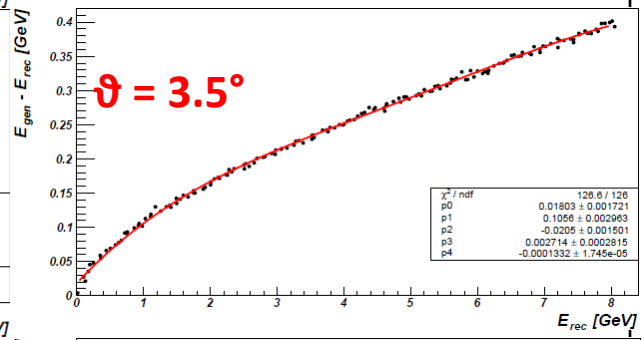
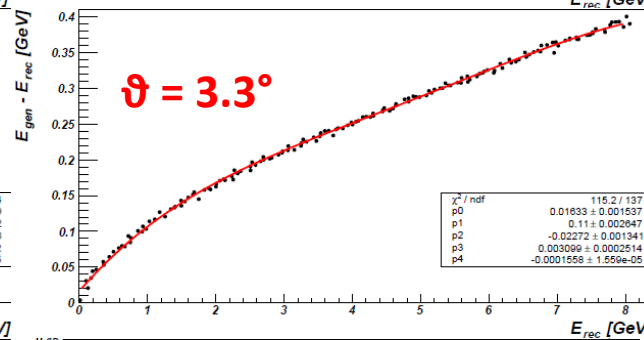
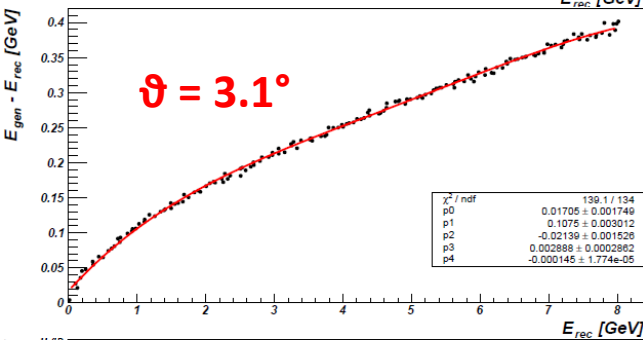
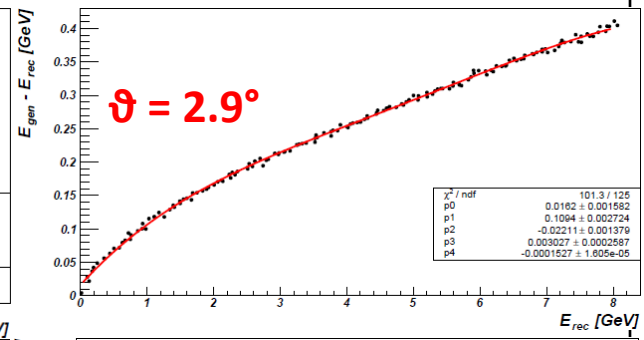
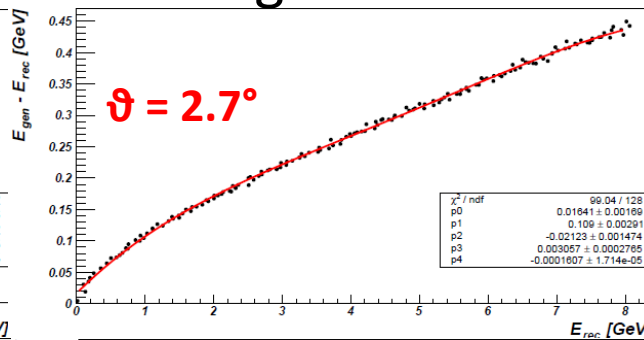
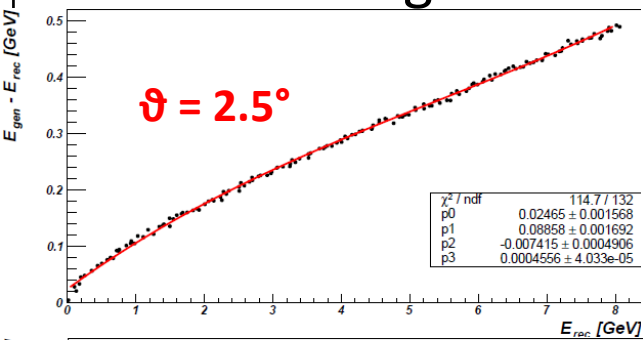
From these fits we can obtain the energy corrections to compensate the difference between $E_{\text{gen}} - E_{\text{rec}}$

Reconstructed threshold

4° degree polynomium

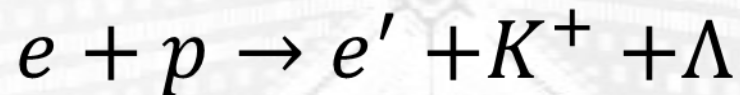
$$f(x) = p_0 + p_1x + p_2x^2 + p_3x^3 + p_4x^4$$

$E_{\text{gen}} - E_{\text{rec}}$ vs E_{gen} for all ϑ values



Simulation and fast mc reconstruction of $K^+\Lambda$ electro-production events in CLAS12 using the Gent RPR-2011 model

- Develop realistic event generator
- Simulation of *quasi-data* events including simplified experimental effects with FASTMC for channel



- Selection of trigger conditions
- Production of events with different run conditions to extract the better configuration.
- Conclusions

Available data on “Strange Calc” web site

StrangeCalc

Reaction type:

- Reaction: $p(e, e'K^+)\Lambda$ $p(e, e'\pi^+)n$
 $p(e, e'K^+)\Sigma^0$ $n(e, e'\pi^-)p$
 $p(e, e'K^0)\Sigma^+$

- Non-interference cross sections: $d\sigma_U$ $d\sigma_L$ $d\sigma_T$
Interference cross sections: $d\sigma_{LT}$ $d\sigma_{TT}$ $d\sigma_{LT'}$ $d\sigma_{TT'}$
Induced recoil polarization: $P_{y'}^0$
 P_n^0
Transferred recoil polarization: $P'_{z'}$ P'_z
 P'_l P'_t

- Energy variable: W s $E_{\gamma, \text{c.m.}}$ $E_{\gamma, \text{lab}}$
 Fixed Range List
 GeV

- Angular variable: $\cos \theta_{\text{c.m.}}$ $-t$ $-u$
 Fixed Range List

- Photon virtuality (Q^2): Fixed Range List
 GeV²

- Model: RPR-2011
 RPR-2007
 VR
 No resonance contributions

$x''y''z''$ -frame: The z'' -axis is along the virtual photon's three-momentum, the $x''z''$ -plane is the electron plane, and the x'' -axis' direction is such that the final electron's x'' -component is positive.

ntl -frame: The l -axis is along the final baryon's three-momentum, the tl -plane is the hadron plane, and the t -axis' direction is such that the virtual photon's t -component is positive.

For the options 'Fixed' and 'Range', unphysical entries will be corrected if the variable's minimum/maximum value is not fixed. E.g.: $W = 0$ GeV will be corrected to $W = W_0$, with W_0 being the threshold energy, and $-t = 0$ GeV² will be corrected to $-t = -t_0$, with $-t_0$ being the minimum value of $-t$.

StrangeCalc data have been used for the Event Generator.

We are in contact with the Gent group to add the hybrid contributions.

RPR-2011 model: Phys. Rev. C **86**, 015212 (2012)
RPR-2007 model: Phys. Rev. C **73**, 045207 (2006) and
Phys. Rev. C **75**, 045204 (2007)
VR model: Phys. Rev. C **89**, 025203 (2014) and
Phys. Rev. C **89**, 065202 (2014)

Trigger conditions and simulations

Step 1

Selection of trigger conditions for fastmc event generator:

- 1 electron in CLAS
 - 1 charged particle in CLAS
- Or
- 1 electron in FT
 - 2 charged particles in CLAS

Charged particle: proton, π^- , k^+

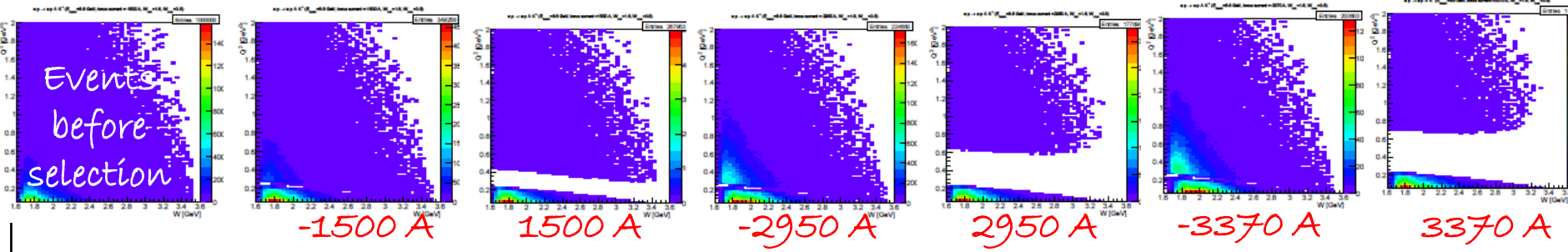
Step 2

Production of plots with the conditions:

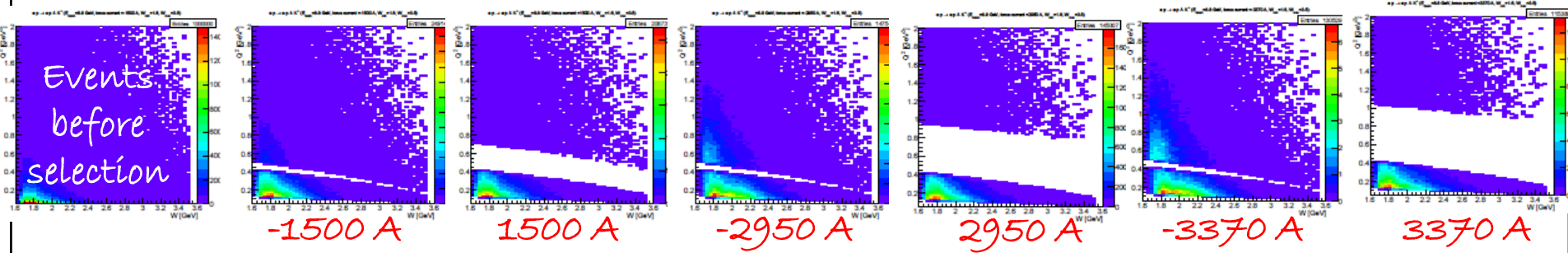
- $E_{\text{beam}} = 6.6 \text{ GeV}, 8.8 \text{ GeV}, 11 \text{ GeV}$
- Torus current = $\pm 1500 \text{ A}, \pm 2950 \text{ A}, \pm 3370 \text{ A}$

Q^2 vs W for different run conditions

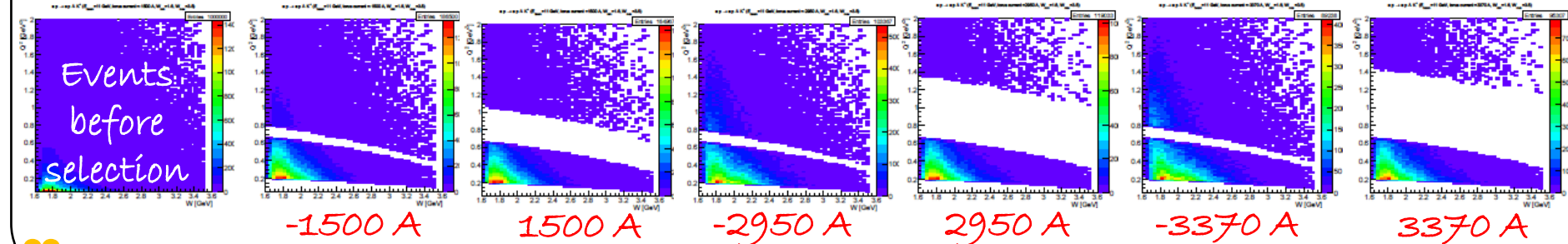
E = 6.6 GeV



E = 8.8 GeV



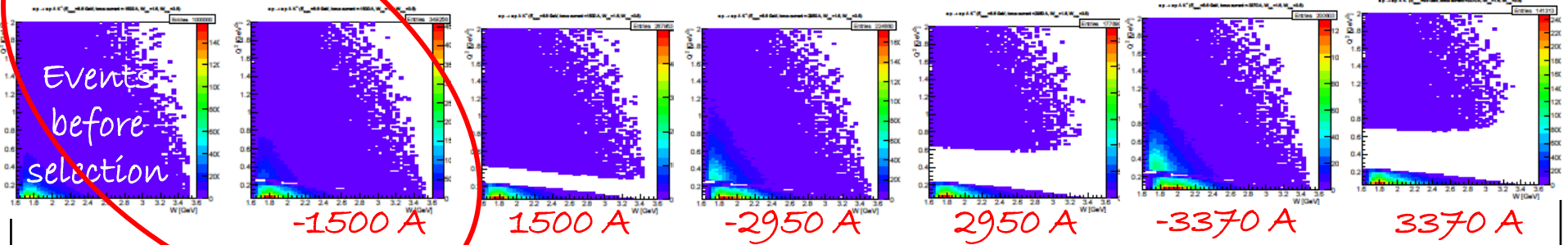
E = 11 GeV



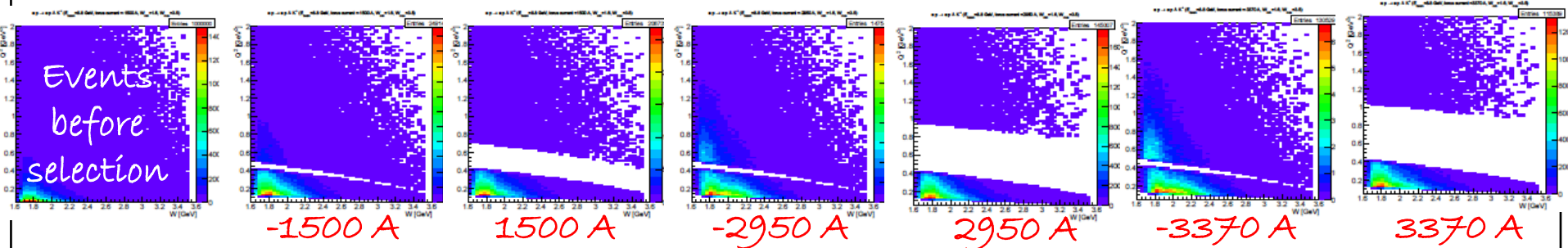
Q^2 vs W for different run conditions

E = 6.6 GeV

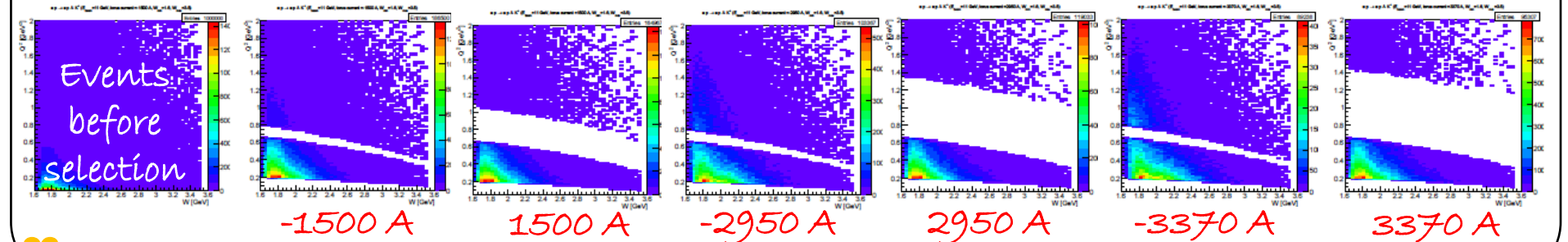
Best efficiency value



E = 8.8 GeV

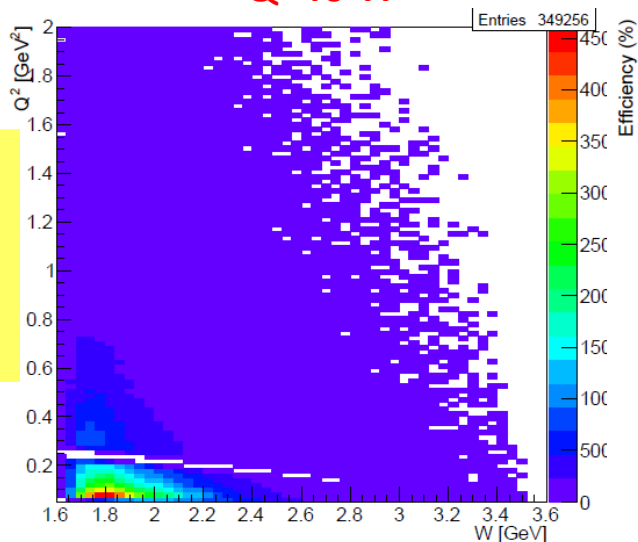


E = 11 GeV

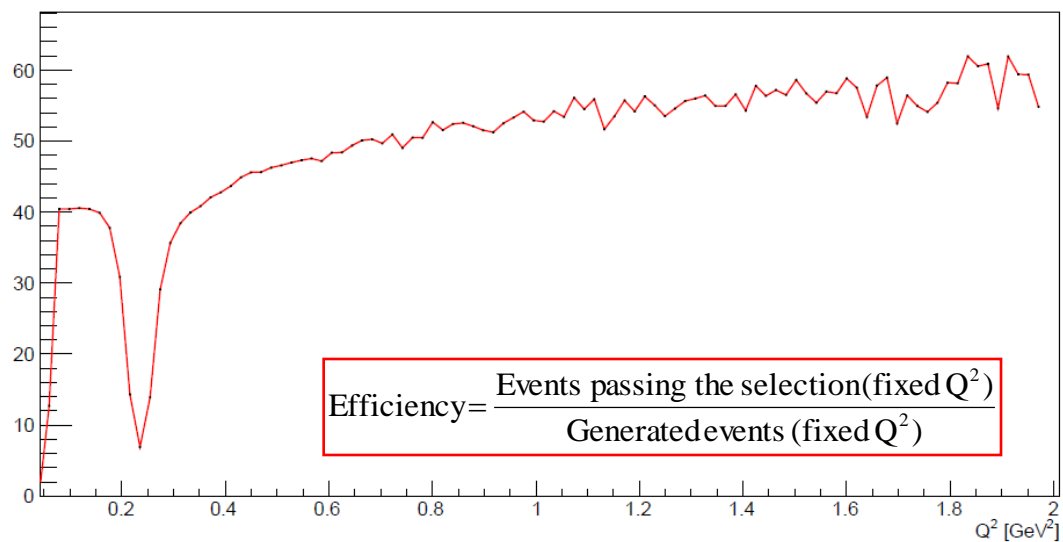


Covering the whole Q^2 range

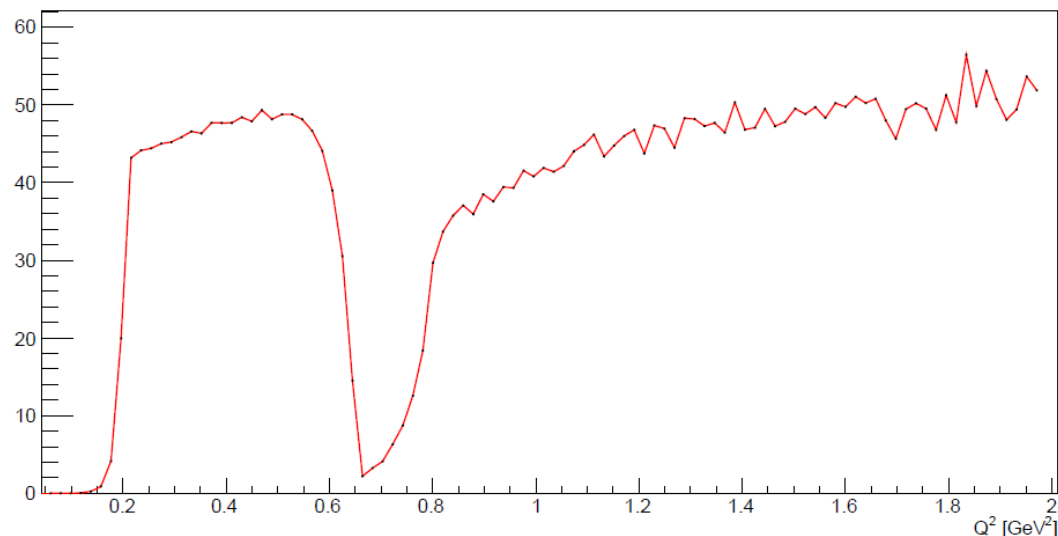
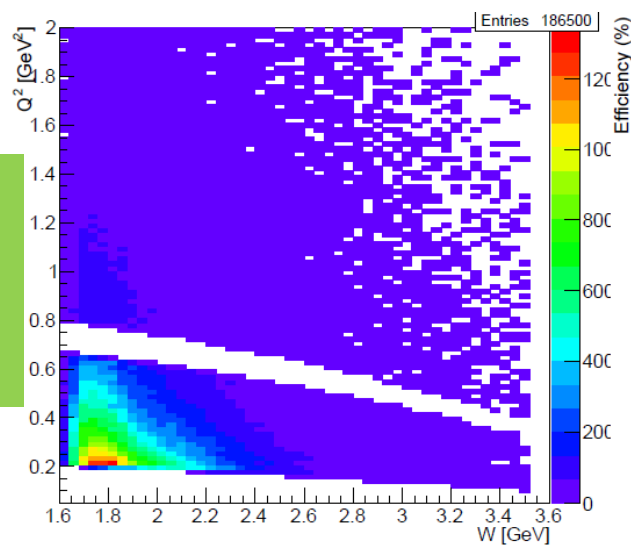
Q^2 vs W



Efficiency curve



Complementary ranges

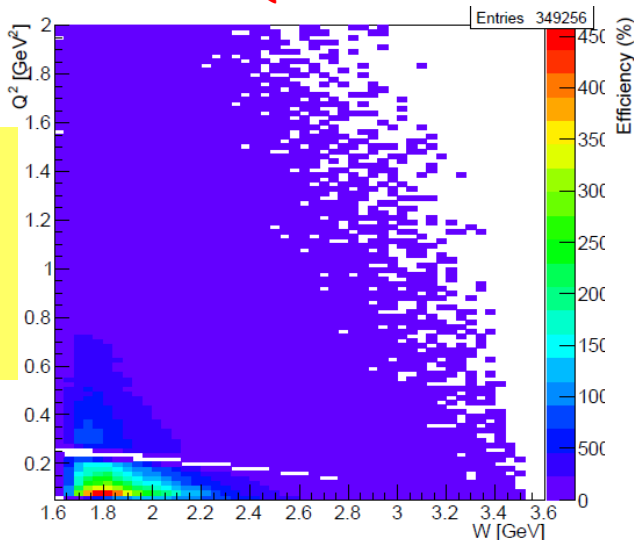


$E =$
6.6 GeV
TorCur=
-1500 A

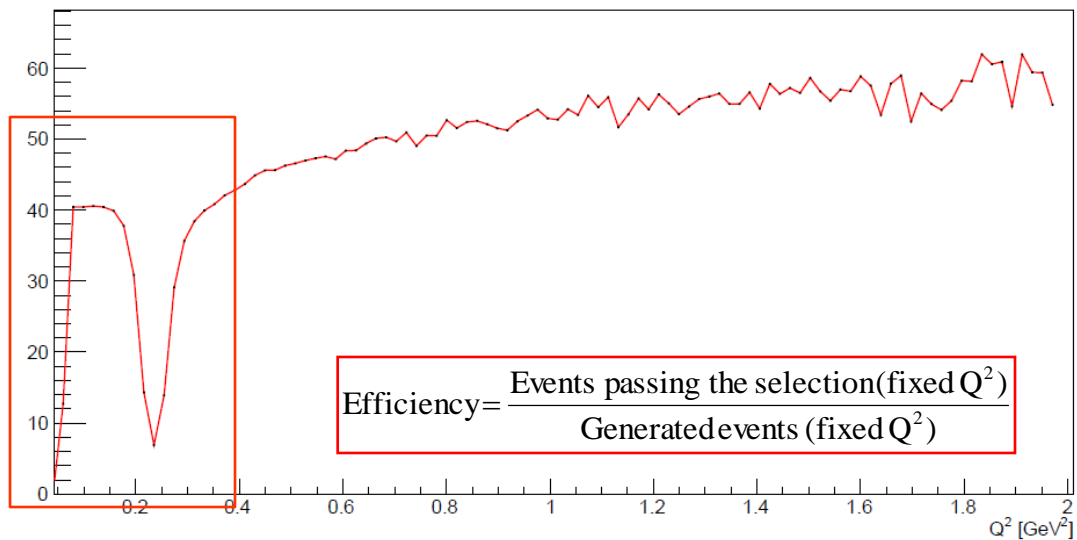
$E =$
11 GeV
TorCur=
-1500 A

Covering the whole Q^2 range

Q^2 vs W

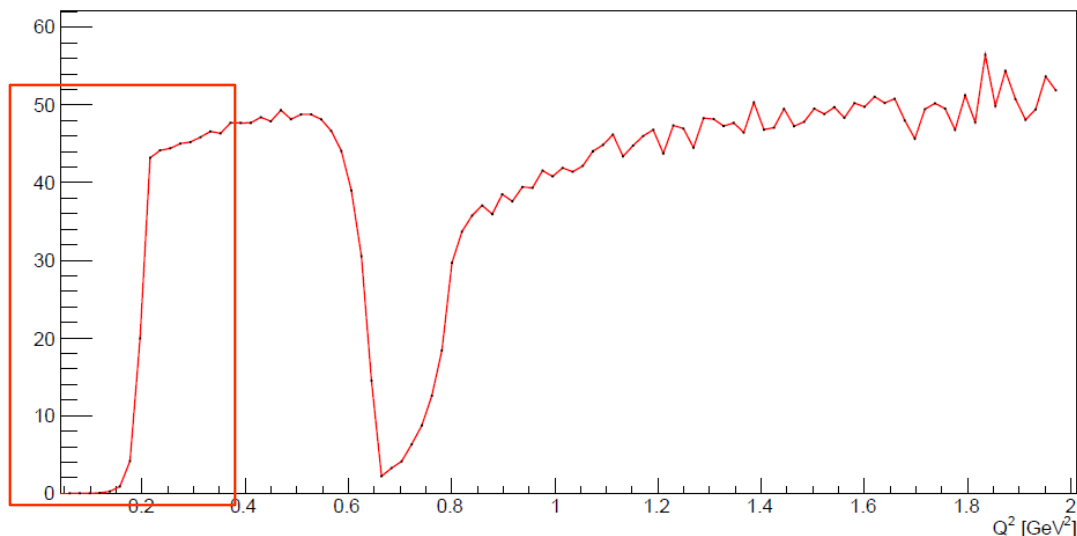
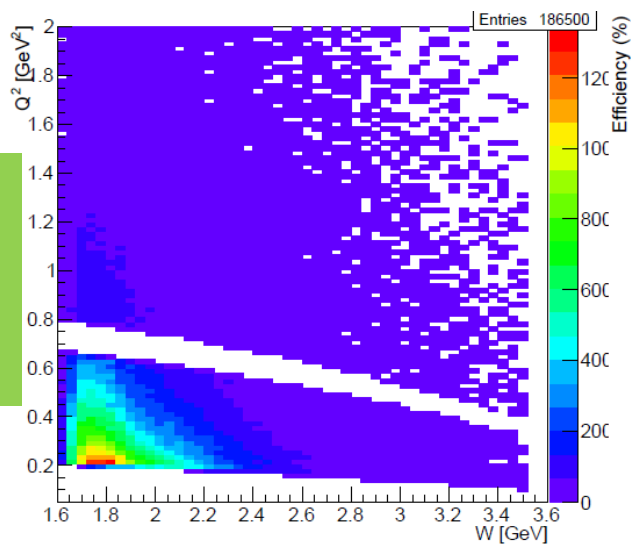


Efficiency curve



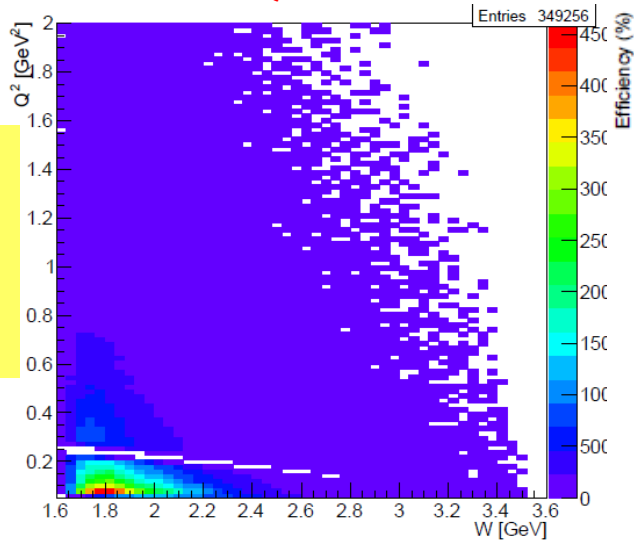
$E =$
6.6 GeV
TorCur=
-1500 A

Complementary ranges

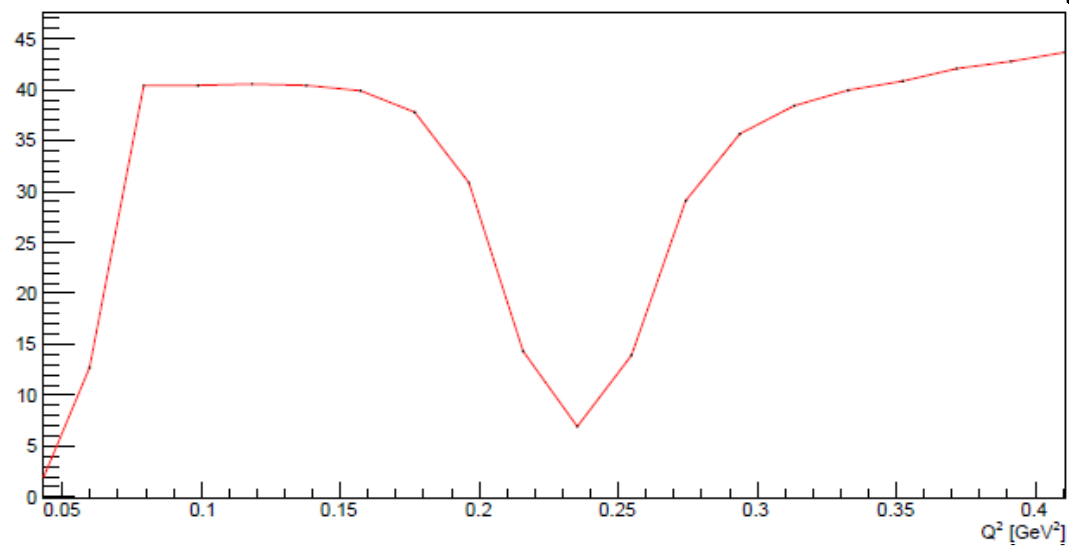


Covering the whole Q^2 range

Q^2 vs W

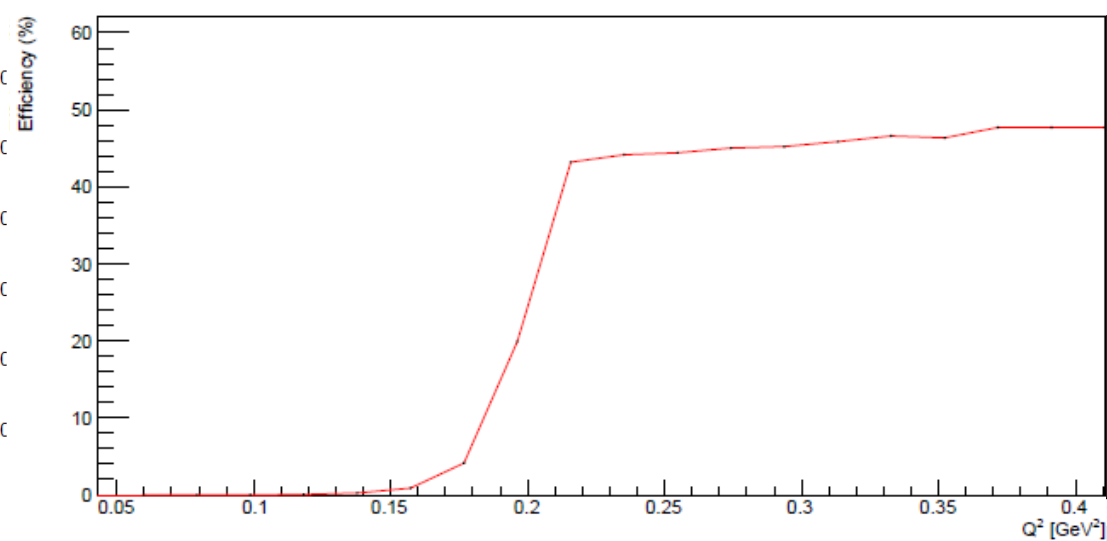
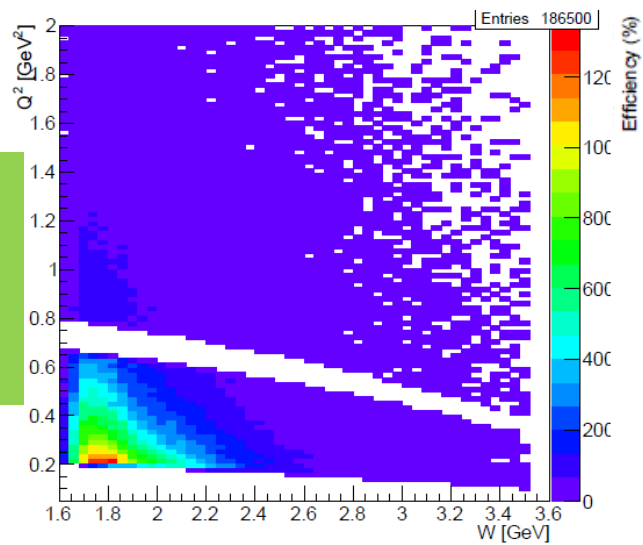


Efficiency curve



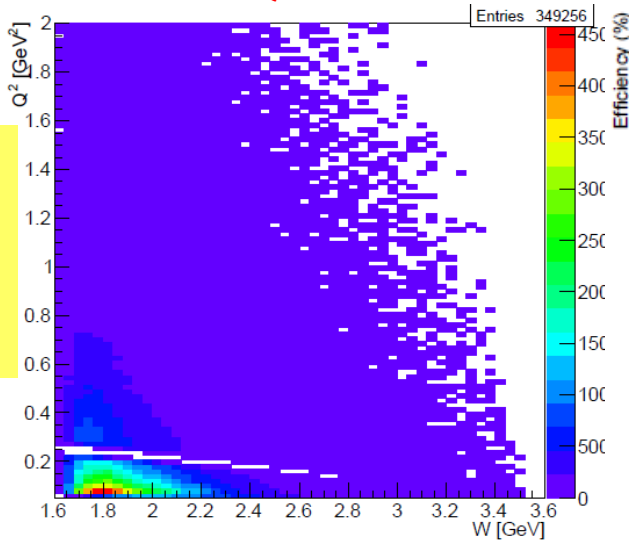
$E =$
6.6 GeV
TorCur=
-1500 A

Complementary ranges



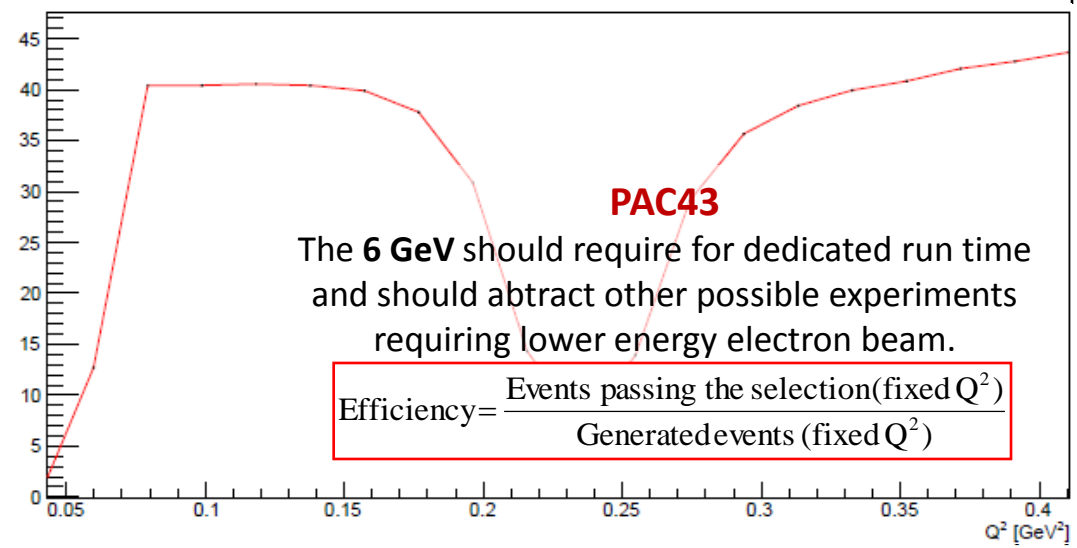
Covering the whole Q^2 range

Q^2 vs W



E =
6.6 GeV
TorCur=
-1500 A

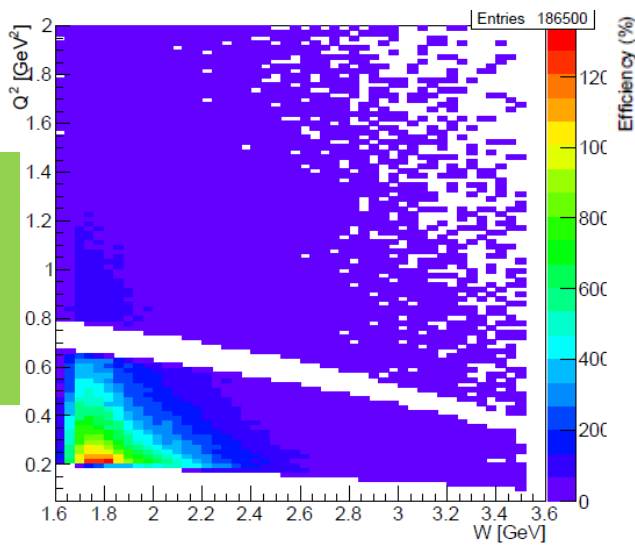
Efficiency curve



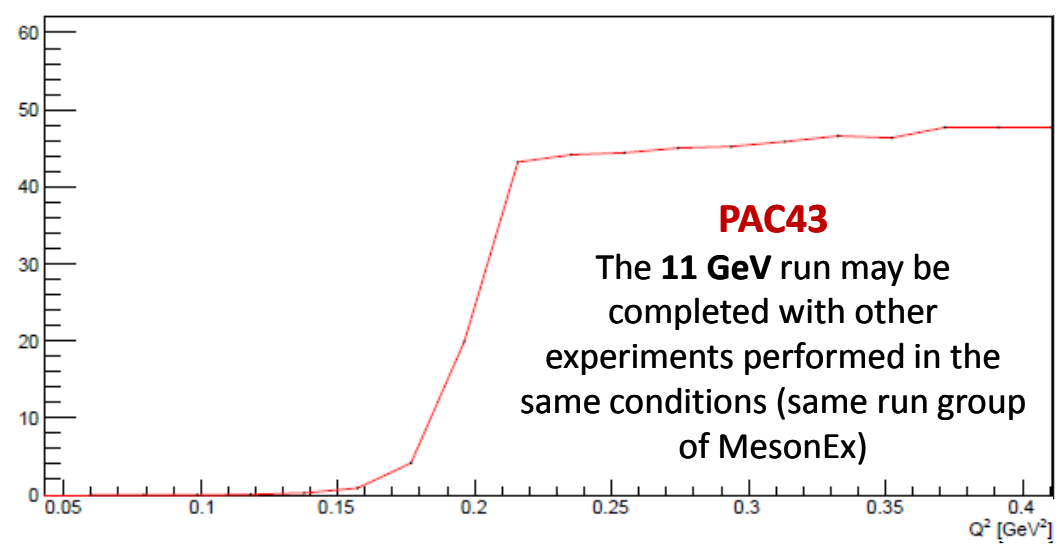
The **6 GeV** should require for dedicated run time and should abstract other possible experiments requiring lower energy electron beam.

$$\text{Efficiency} = \frac{\text{Events passing the selection (fixed } Q^2)}{\text{Generated events (fixed } Q^2)}$$

Complementary ranges



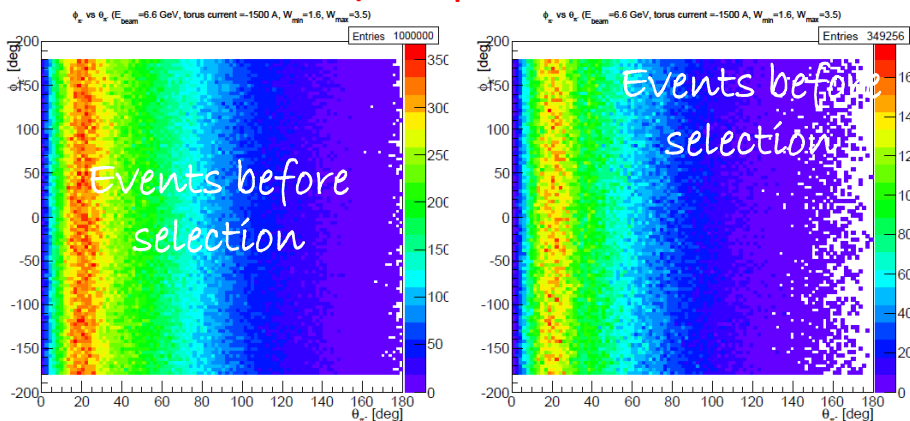
E =
11 GeV
TorCur=
-1500 A



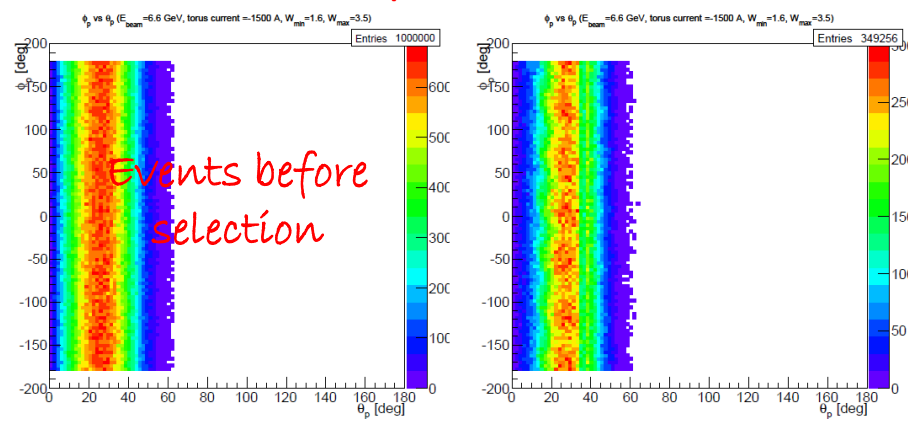
The **11 GeV** run may be completed with other experiments performed in the same conditions (same run group of MesonEx)

Results for run conditions: $E_{\text{beam}}=6.6$ GeV TorCur=-1500 A

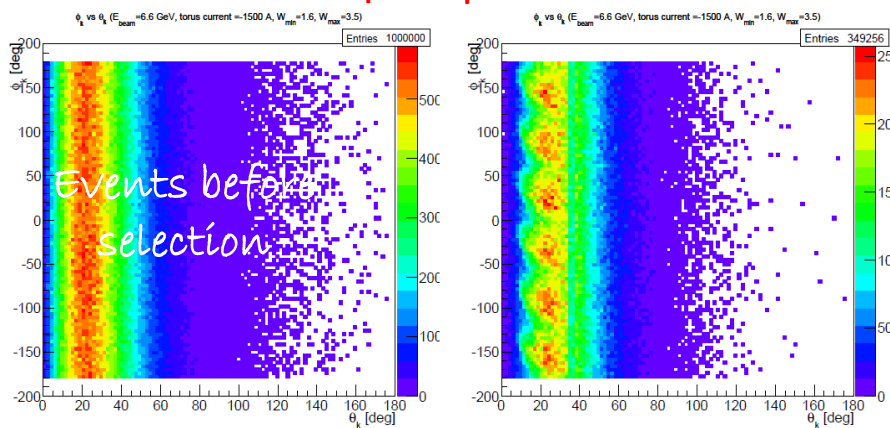
ϑ vs ϕ for proton



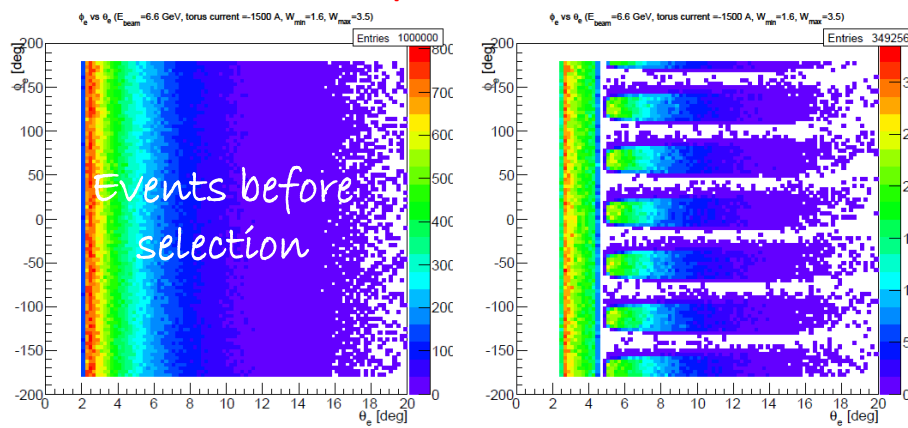
ϑ vs ϕ for kaon



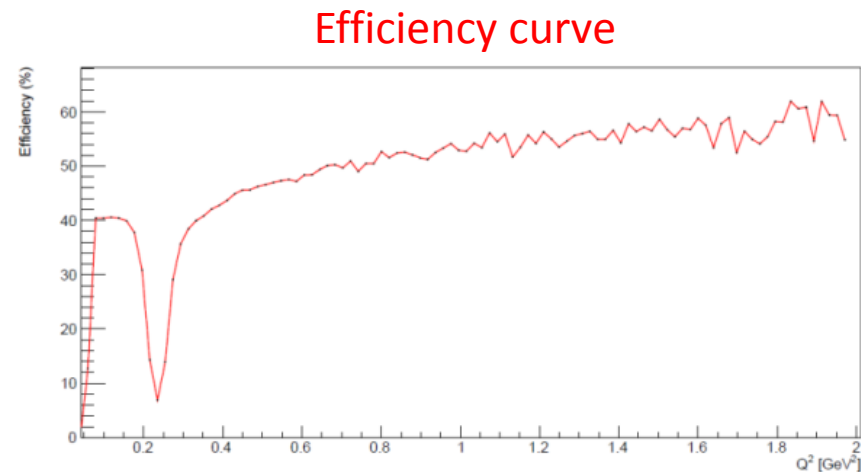
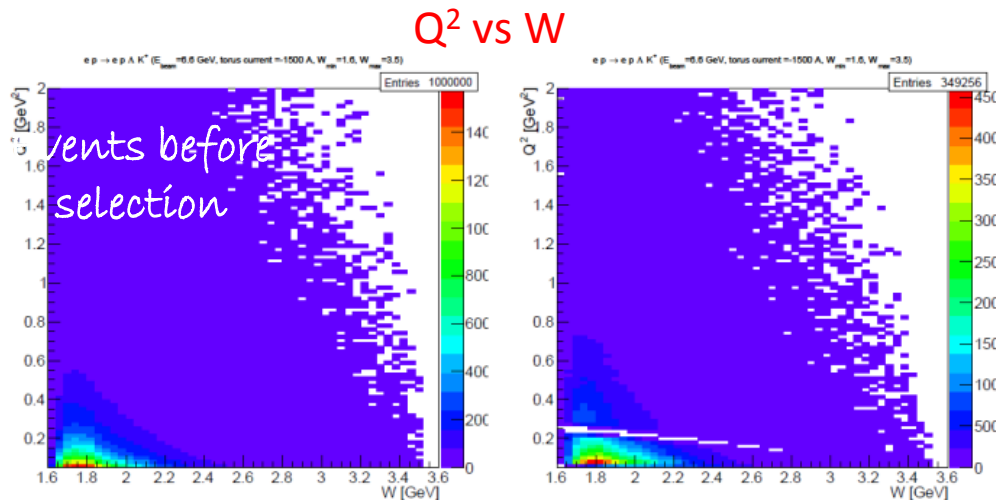
ϑ vs ϕ for pion



ϑ vs ϕ for electron



Results for run conditions: $E_{\text{beam}}=6.6 \text{ GeV}$ TorCur=-1500 A



A Letter of Intent has been endorsed by the PAC43.

A Letter of Intent to the Jefferson Lab PAC43

Search for Hybrid Baryons with CLAS12 in Hall B

A. D'Angelo,^{1,2} I. Balossino,¹¹ L. Barion,¹¹ M. Battaglieri,³ V. Bellini,¹² V.D. Burkert,⁴ S. Capstick,⁵ D. Carman,⁴
 A. Celentano,³ G. Ciulli,¹¹ M. Contalbrigo,¹¹ V. Credé,⁵ R. De Vita,³ E. Fanchini,³ G. Fedotov,⁶ A. Filippi,¹⁰
 E. Golovach,⁶ R. Gothe,⁷ B.S. Ishkhanov,^{6,13} E.L. Isupov,⁶ V.P. Koubarovski,⁴ L. Lanza,² P. Lenisa,¹¹ F.
 Mammoliti,¹² V. Mokeev,^{4,6} A. Movsisyan,¹¹ M. Osipenko,³ L. Pappalardo,¹¹ M. Ripani,³ A. Rizzo,² J. Ryckebusch,⁸
 Iu. Skorodumina,^{7,13} C. Sutera,¹² A. Szczepaniak,^{9,4} M. Taiuti,³ M. Turisini,¹¹ M. Ungaro,⁴ and V. Ziegler⁴

Conclusions

Cluster reconstruction algorithm

- Studies have been performed regarding the dependence of cluster reconstruction on the polar angle
- Calibration corrections have been obtained, for Energy range [0.1, 8] GeV and for theta values in the range [2.5, 4.5]° with steps of 0.2°.

Simulation and fast mc reconstruction of $K^+\Lambda$ electro-production events in CLAS12

- Run condition: $E_{\text{beam}}=6.6$ GeV and Torus Current = -1500 A presents good values of efficiency with respect to the other ones
- Search of hybrid baryons in runs with standard conditions of magnet and beam energy can be integrated with dedicated runs.

Future Work

Next step: Full Proposal

- Inclusion of an “hybrid baryon” contribution to the cross section
- Full implementation in CLAS12 simulation and reconstruction
- Reconstruction of the interaction strength from simulated data

Future Work

Next step: Full Proposal

- Inclusion of an “hybrid baryon” contribution to the cross section
- Full implementation in CLAS12 simulation and reconstruction
- Reconstruction of the interaction strength from simulated data

Thank you

Bibliography

- *CLAS12 Forward Tagger (FT) Technical Design Report*, The CLAS12 Collaboration
- *Draft CLAS-Note, An Inner Calorimeter for CLAS/DVCS experiments*, I. Bedlinskiy, et al.
- *CLAS/DVCS Inner Calorimeter Calibration*, R. Niyazov , S. Stepanyan
- *A Letter of Intent to the Jefferson Lab PAC43, Search for Hybrid Baryons with CLAS12 in Hall B*, A. D'Angelo et al.
- J. Dudek et al., 2012
- V. Moiseev et al., 2012, *Experimental study of the P11(1440) and D13(1520) resonances from the CLAS data on $ep \rightarrow e\pi^+\pi^- p$*
- I. G. Aznauryan et al., CLAS Collaboration, PHYSICAL REVIEW C 80, 055203 (2009)
- [1] S. Capstick and B. D. Keister, Phys. Rev. D 51, 3598 (1995)
- [2] I. G. Aznauryan, Phys. Rev. C 76, 025212 (2007).
- [3] Z. P. Li, V. Burkert, and Zh. Li, Phys. Rev. D 46, 70 (1992).

The Forward Tagger (FT)

For $Q^2 \approx 0$ the exchanged virtual photon becomes for all practical purposes almost a real photon

$$Q^2 = -q^2 = -(\mathbf{p}_e - \mathbf{p}_{e'})^2 = m_{\gamma^*}^2 c^4 = 2E_e E_{e'} + m_e^2 + m_{e'}^2 - 2\mathbf{p}_e \mathbf{p}_{e'} = 2(E_e E_{e'} - |\mathbf{p}_e| |\mathbf{p}_{e'}| \cos \vartheta) = 2E_e E_{e'} (1 - \cos \vartheta)$$

Where

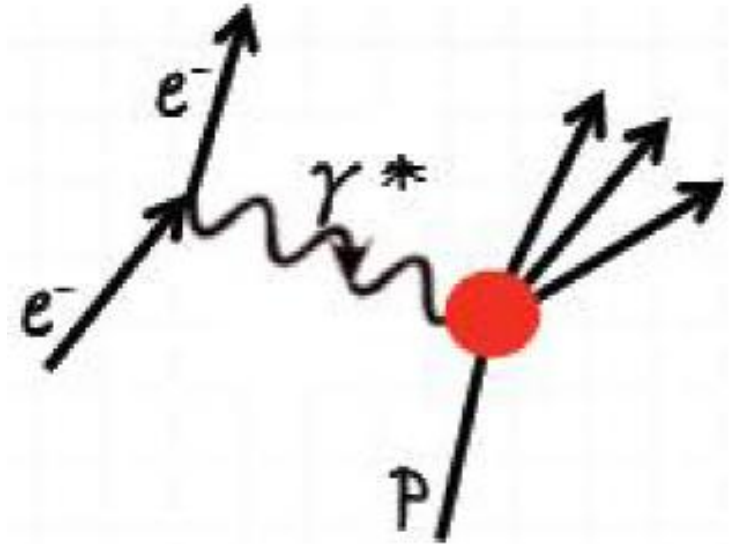
$$q = \mathbf{p}_e - \mathbf{p}_{e'}$$

Using the prosthaphaeresis formula:

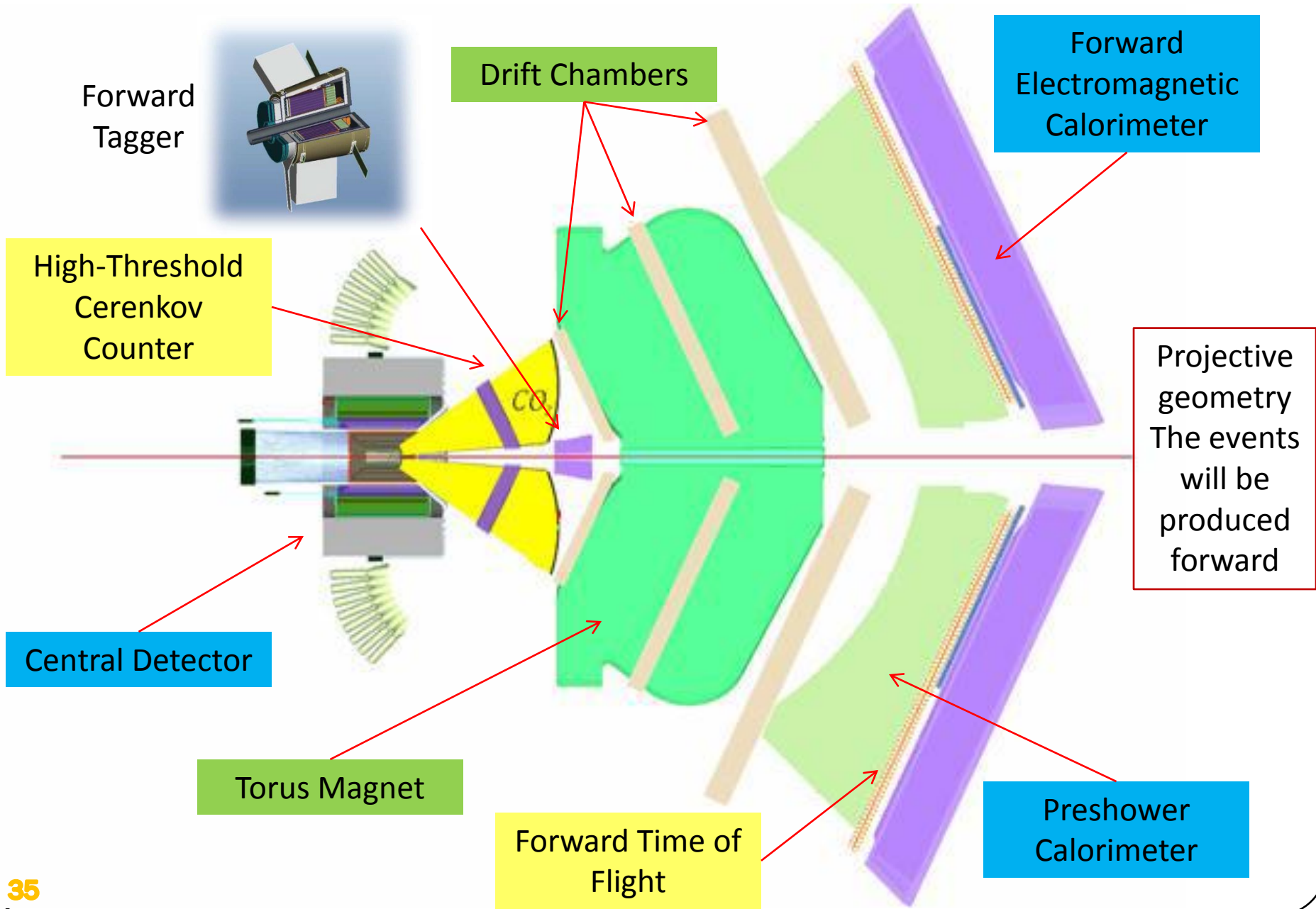
$$Q^2 = 4E_{Beam} E_{e'} \sin^2 \frac{\vartheta}{2}$$

Where ϑ is the angle between the e and the e' directions.

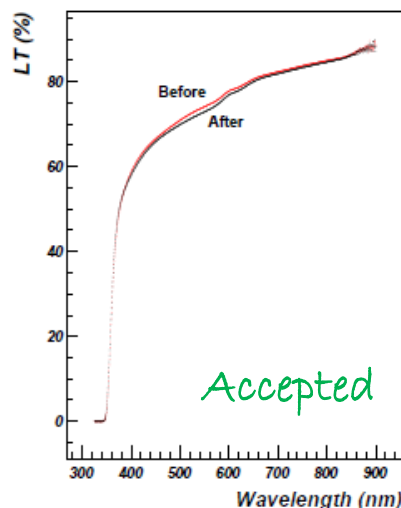
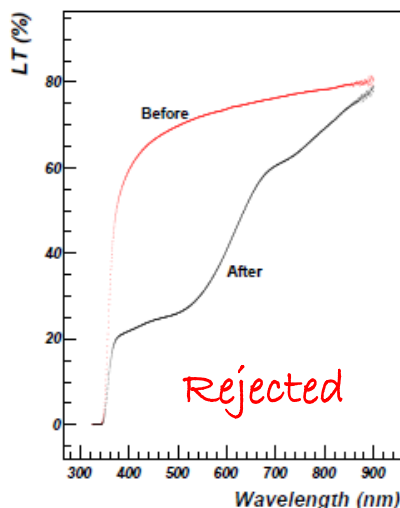
To select events where a quasi-real photon has been exchanged, electrons scattered with a small ($\vartheta < 5^\circ$) must be detected and measured \rightarrow **Forward Tagger (FT)** apparatus



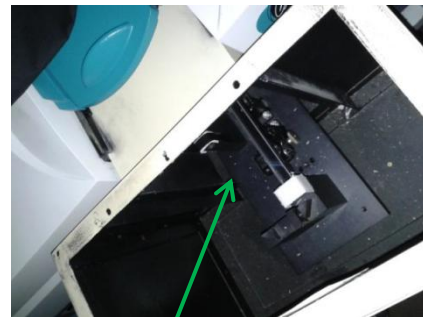
Experimental setup: CLAS12



Light Transmission of PWO crystals for EM calorimetry in the CLAS12 FT



Giessen measurements: employment of a **spectrophotometer** to perform hardness tests – LT before and after irradiation- on the **332 PWO crystals** that compose the FT calorimeter.

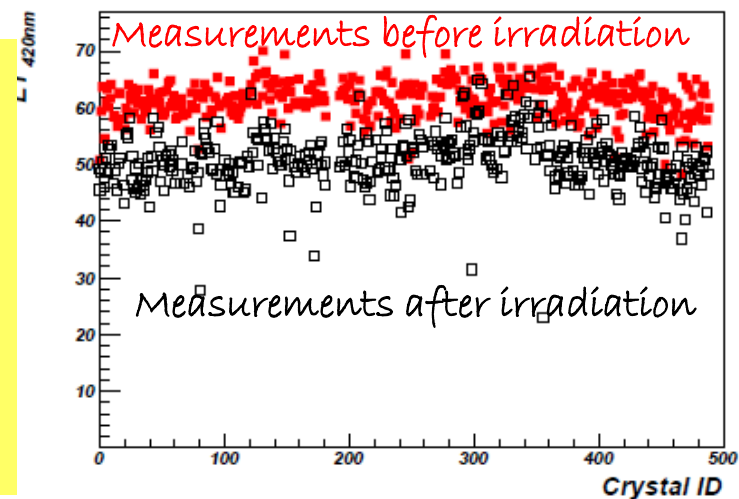


SICCAS 20 cm PbWO₄

For each of the **332 crystals**:

- Measurement in the spectrophotometer before irradiation
- Irradiation (dose of a month operations at CLAS12)
- 30 minutes in a dark environment for the fast component of the crystal's light transmission to occur
- Measurement in the spectrophotometer after irradiation
- Data analysis and evaluation of quality on the basis of

Absorption coefficient:
$$\Delta k = \frac{1}{\text{length}} \ln \frac{T_{\text{before}}}{T_{\text{after}}}$$



NIM paper:

Assessing the performance under ionising radiation of lead tungstate scintillators for EM calorimetry in the CLAS12 Forward Tagger

S. Fegan^{a,*}, E. Auffray^b, M. Battaglieri^a, E. Buchanan^c, B. Caiffi^a, A. Celentano^a, L. Colaneri^d, A. D'Angelo^d, R. De Vita^a, V. Dormenev^e, E. Fanchini^a, L. Lanza^d, R.W. Novotny^e, F. Parodi^a, A. Rizzo^d, D. Sokhan^c, I. Tarasov^f, I. Zonta^d

Light Transmission of PWO crystals for EM calorimetry in the CLAS12 FT

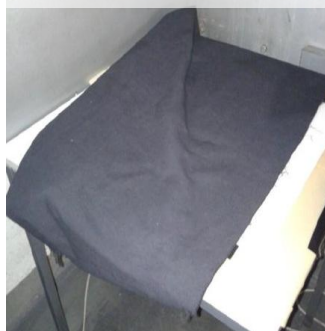
Giessen measurements: employment of a **spectrophotometer** to perform hardness tests –LT before and after irradiation- on the **332 PWO crystals** that compose the FT calorimeter.

Spectrophotometer



SICCAS 20 cm
PbWO₄

Black Cloath



Irradiation Chamber

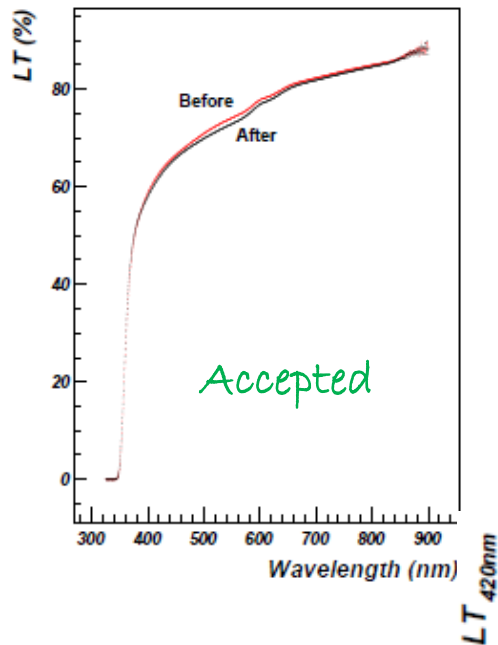


For each of the **332 crystals**:

- Measurement in the spectrophotometer before irradiation
- Irradiation (dose of a month operations at CLAS12)
- 30 minutes in a dark environment for the fast component of the crystal's light transmission to occur
- Measurement in the spectrophotometer after irradiation
- Data analysis and evaluation of quality on the basis of

Absorption coefficient: $\Delta k = \frac{1}{length} \ln \frac{T_{before}}{T_{after}}$

Light Transmission of PWO crystals for EM calorimetry in the CLAS12 FT



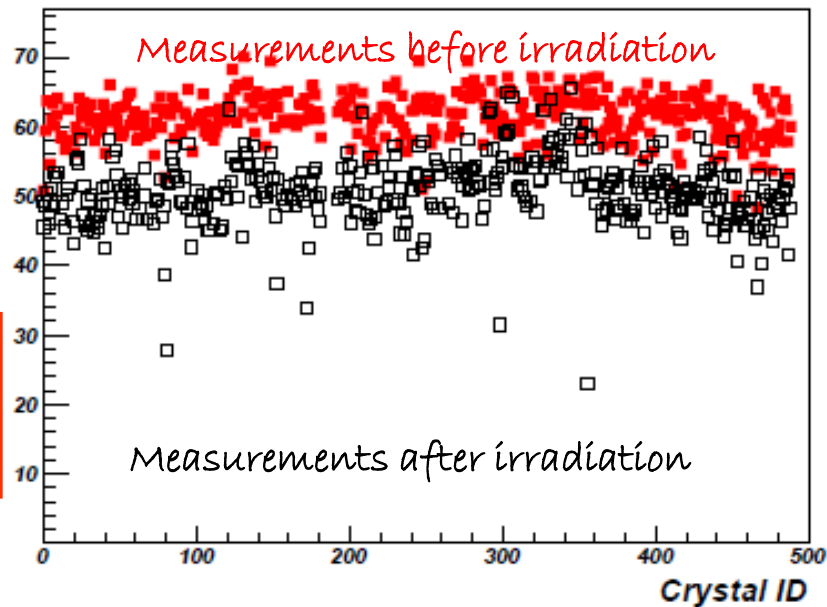
The absorption coefficient $\Delta k[\text{m}^{-1}]$ quantifies the absorption

$$\Delta k = \frac{1}{\text{length}} \ln \frac{T_{\text{before}}}{T_{\text{after}}}$$

NIM paper, S. Fegan et al., Sec. A, volume 789, 21 July 2015, Pages 101-108

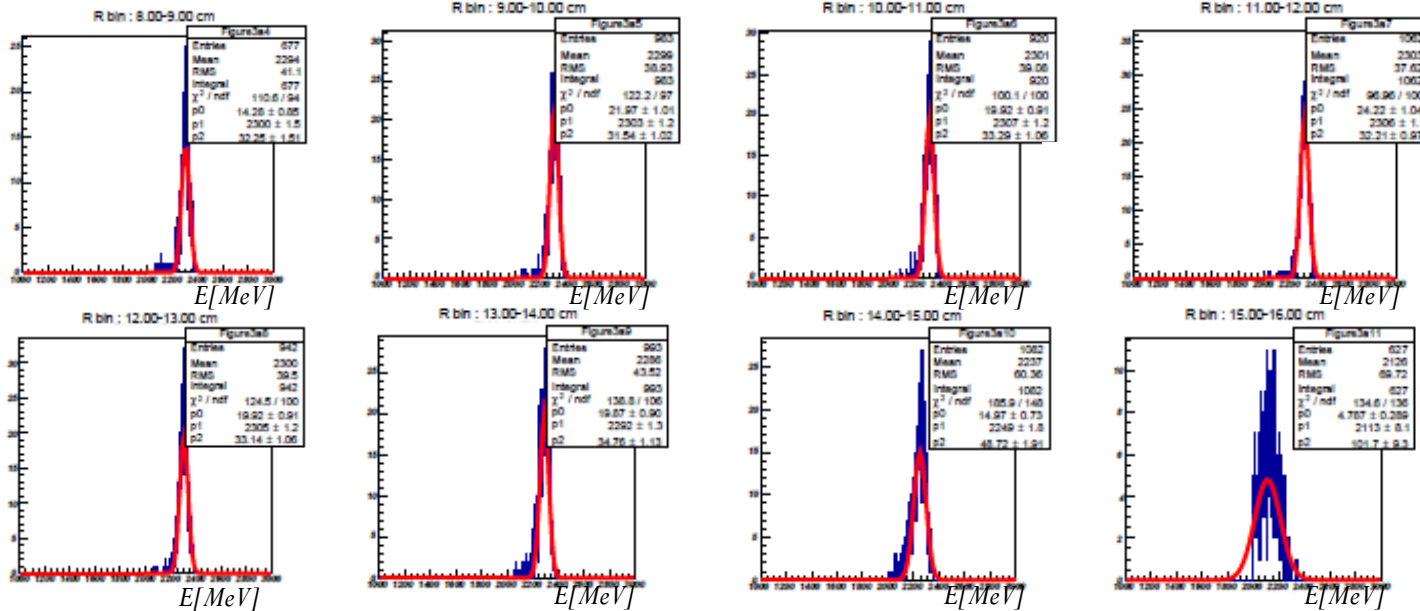
Assessing the performance under ionising radiation of lead tungstate scintillators for EM calorimetry in the CLAS12 Forward Tagger

S. Fegan^{a,*}, E. Auffray^b, M. Battaglieri^a, E. Buchanan^c, B. Caiffi^a, A. Celentano^a, L. Colaneri^d, A. D'Angelo^d, R. De Vita^a, V. Dormenev^e, E. Fanchini^a, **L. Lanza**, R.W. Novotny^e, F. Parodi^a, A. Rizzo^d, D. Sokhan^c, I. Tarasov^f, I. Zonta^d



Single photon reconstruction

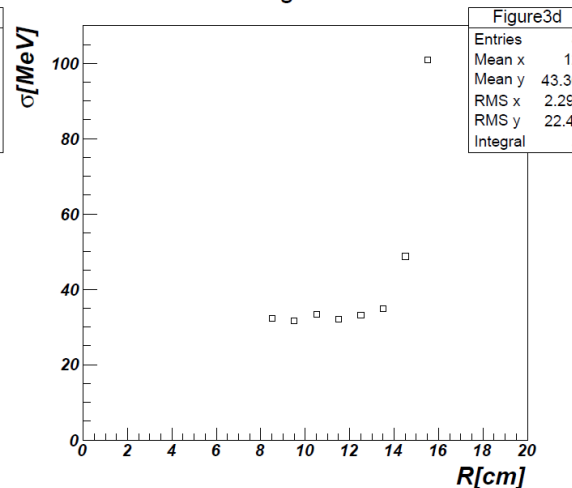
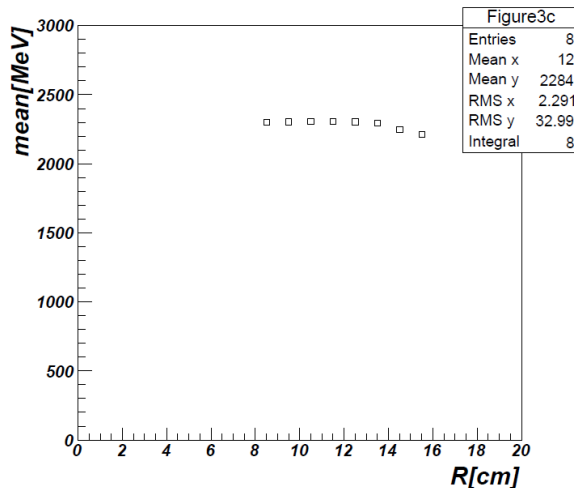
Reconstructed cluster energy slices for $E_{gen}^{\gamma} = 2.5$ GeV



E_{clust} sliced with R bins and fitted with gaussian

mean 6

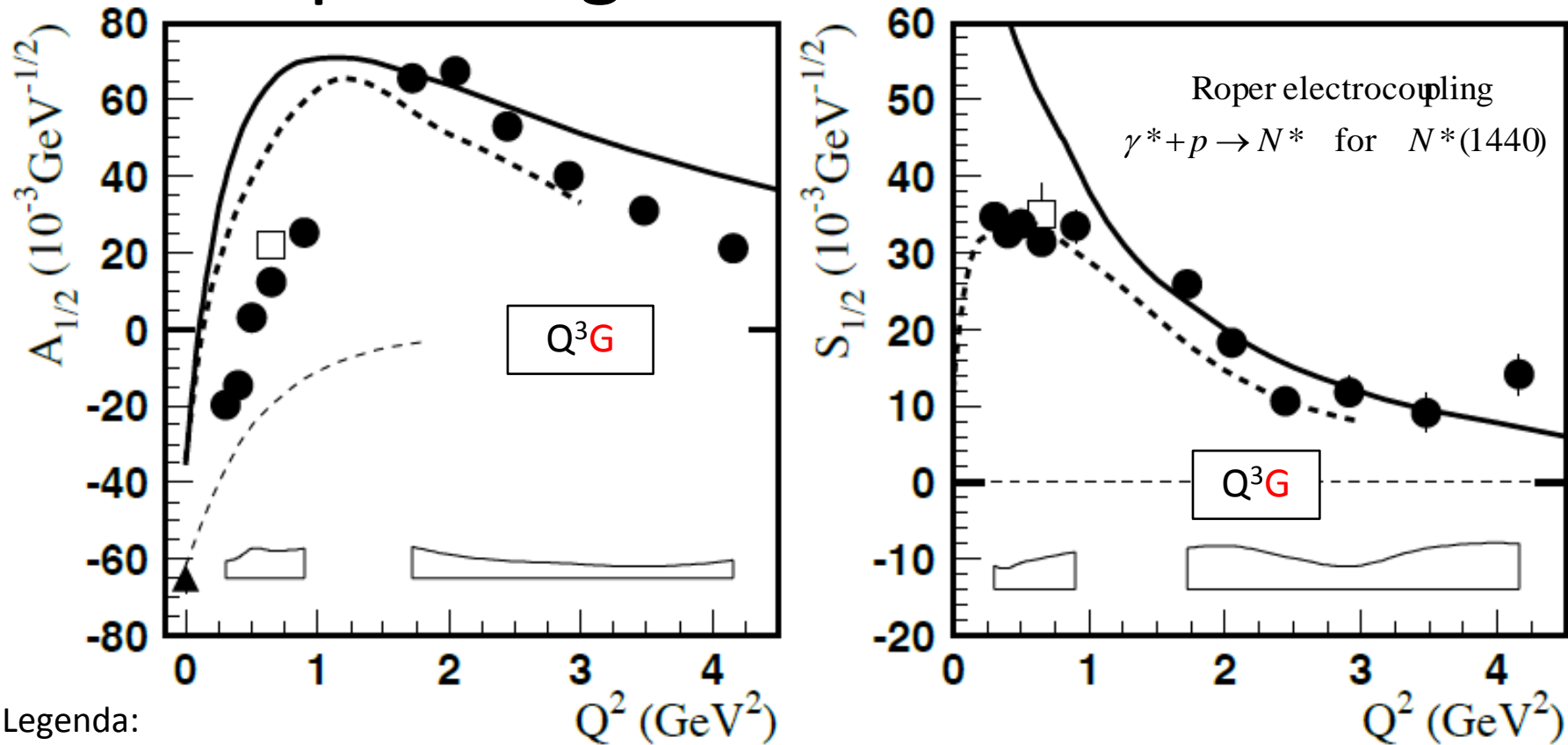
sigma 6



mean
from the
fit as a
function
of R

σ
from the
fit as a
function
of R

Separating Q^3G from Q^3 states



Legenda:

- results from Table IX obtained from CLAS data in [I. G. Aznauryan et al., (2009)]
- results of the combined analysis of CLAS single π and 2π electroproduction data
- ▲ at $Q^2 = 0$ is the RPP estimate

The bands show the model uncertainties.

----- — results obtained in the LF relativistic quark models assuming that $N(1440)P_{11}$ is a first radial excitation of the $3q$ ground state: [1] (-----), [2] (—).

The thin dashed curves are obtained assuming that $N(1440)P_{11}$ is a gluonic baryon excitation ($q3G$ hybrid state) [3].

Separating $Q^3 G$ from Q^3 states: $A_{1/2}(Q^2)$ and $S_{1/2}(Q^2)$

The N^* hadronic decay amplitudes can be expanded in partial waves of total momentum J

$$\langle \lambda_f | T_{dec} | \lambda_R \rangle = \langle \lambda_f | T_{dec}^{J_r} | \lambda_R \rangle d_{\mu\nu}^{J_r}(\cos \theta^*) e^{i\mu\phi^*}$$

$\nu = -\lambda_\Delta$
 CM polar and azimuthal angles for the final K
 λ_R

where

$$\langle \lambda_f | T_{dec}^{J_r} | \lambda_R \rangle = \frac{2\sqrt{2\pi} \sqrt{2J_r + 1} M_r \sqrt{\Gamma_{\lambda_f}}}{\sqrt{\langle p_i^r \rangle}} \sqrt{\frac{\langle p_K^r \rangle}{\langle p_K \rangle}}$$

N^* spin
 partial hadronic decay widths of the N^* to $K\Lambda$ final states f of helicity λ_f
 Magnitudes of the three-momenta of the final K for the $N^* \rightarrow K\Lambda$ decay, evaluated at $W = M_r$ and at the running W , respectively, and averaged over the running mass of the unstable hadron in the intermediate state

The resonance electroexcitation amplitudes can be related to the $\gamma_N NN^*$ electrocouplings $A_{1/2}$, $A_{3/2}$, and $S_{1/2}$ for nucleons

$$\langle \lambda_R | T_{em} | \lambda_\gamma \lambda_p \rangle = \frac{W}{M_r} \sqrt{\frac{8M_N M_r q_{\gamma r}}{4\pi\alpha}} \sqrt{\frac{q_{\gamma r}}{q_\gamma}} A_{1/2,3/2}(Q^2) \quad \text{with} \quad |\lambda_\gamma - \lambda_p| = \frac{1}{2}, \frac{3}{2} \quad \text{for transverse photons,}$$

$$\langle \lambda_R | T_{em} | \lambda_\gamma \lambda_p \rangle = \frac{W}{M_r} \sqrt{\frac{16M_N M_r q_{\gamma r}}{4\pi\alpha}} \sqrt{\frac{q_{\gamma r}}{q_\gamma}} S_{1/2}(Q^2) \quad \text{for longitudinal photons}$$

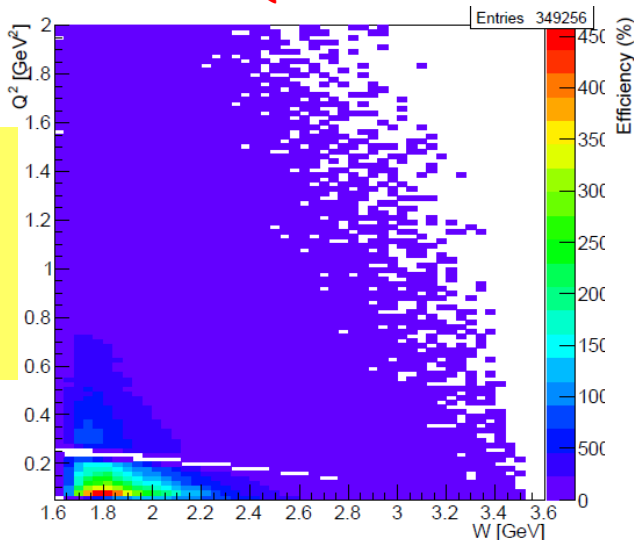
$q_{\nu,r}$ is the three-momentum modulus of the photon at $W =$

$$q_\gamma = \sqrt{Q^2 + E_\gamma^2}$$

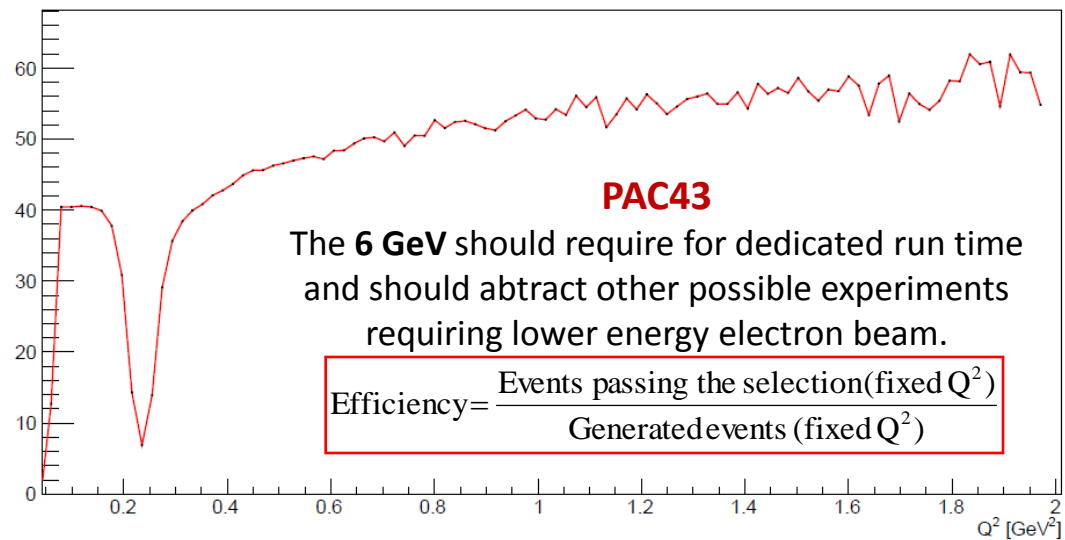
M_r in the CM frame

Covering the whole Q^2 range

Q^2 vs W

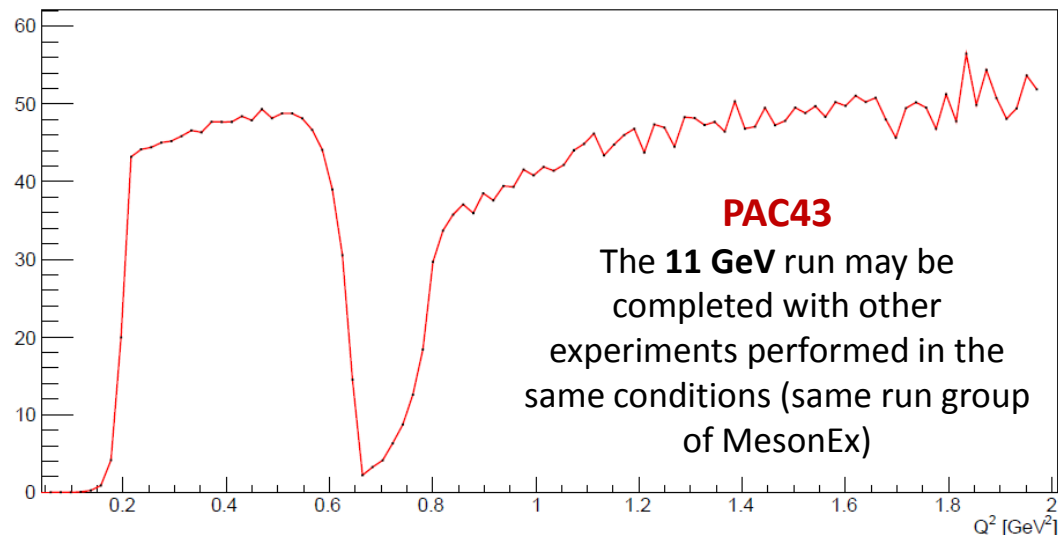
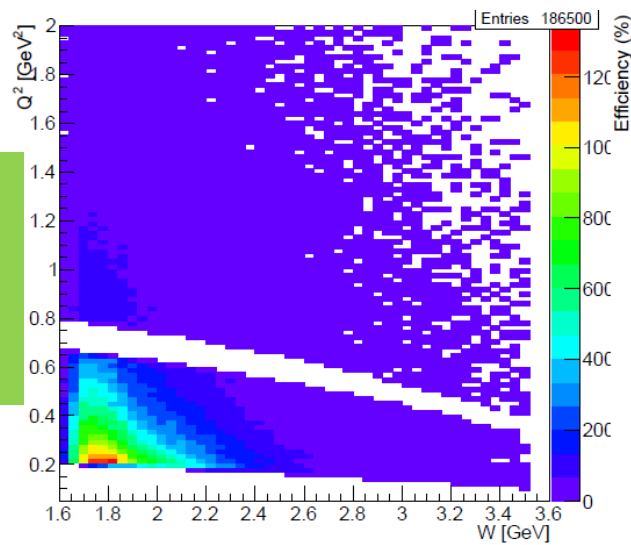


Efficiency curve



Complementary ranges

E =
6.6 GeV
TorCur=
-1500 A

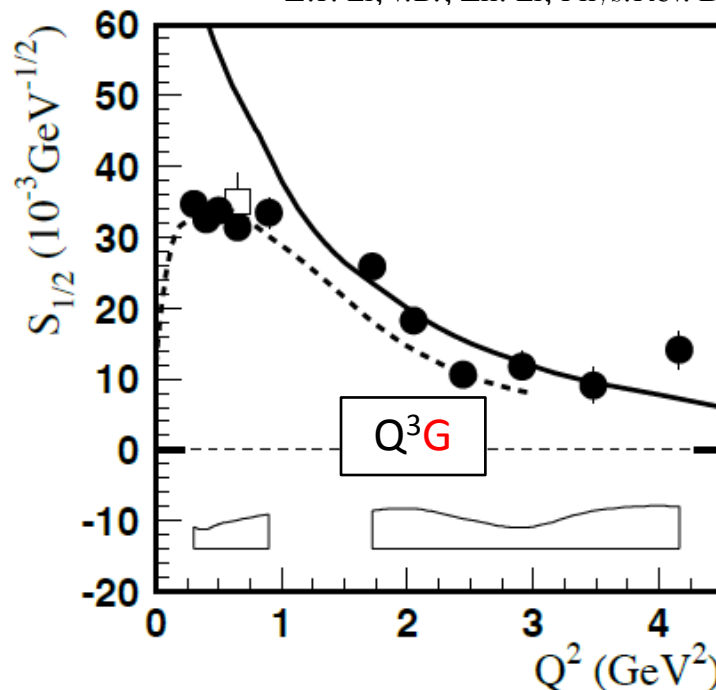
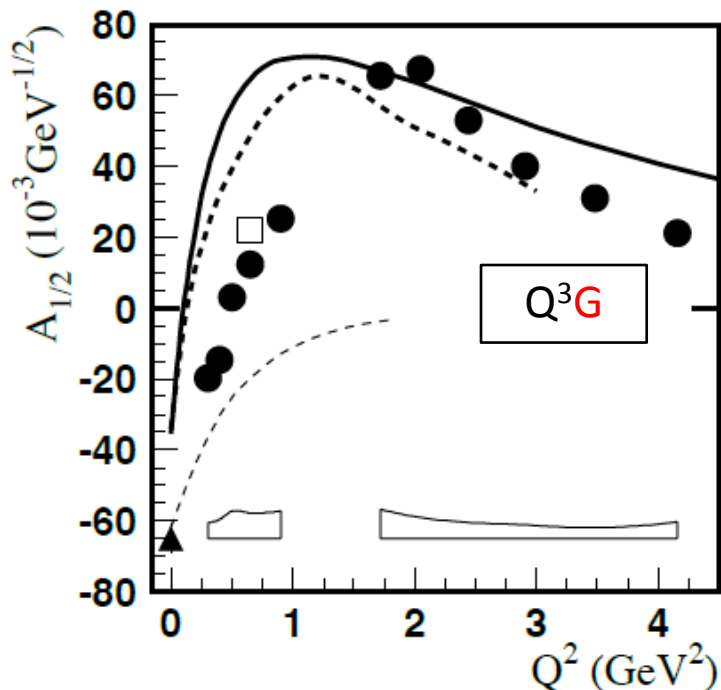


Separating Q^3G from Q^3 states

Transverse elicity amplitude $A_{1/2}(Q^2)$ and longitudinal elicity amplitude $S_{1/2}(Q^2)$ allow to distinguish Q^3G from Q^3 states

$$A_{1/2}^p = \begin{cases} -\frac{2\sqrt{2}}{9} \delta \sqrt{\pi/k_0 \mu_0} \frac{k}{\gamma^2} e^{-k^2/6\alpha_h^2 \gamma^2} & S_{1/2}^p(q^3) = 0 \\ -\frac{\sqrt{2}}{9\sqrt{3}} \sqrt{\pi/k_0 \mu_0} \frac{k}{\gamma^2} \frac{k^2}{\alpha^2 \gamma^2} e^{-k^2/6\alpha^2} & S_{1/2}^p(q^3) = -\frac{1}{3\sqrt{3}} \sqrt{2\pi/k_0 m_q \mu_p} \frac{k^2}{\alpha^2} e^{-k^2/6\alpha^2} \end{cases} \text{ for } \begin{cases} |q^3G\rangle \\ |q^3\rangle \end{cases}$$

Z.P. Li, V.B., Zh. Li, Phys.Rev. D46 (1992) 70



Helicity amplitudes for the $\gamma * p \rightarrow N(1440)P_{11}$ transition. The full circles are the results from Table IX obtained in this work from CLAS data (Tables I–IV). The bands show the model uncertainties. The open boxes are the results of the combined analysis of CLAS single π and 2π electroproduction data [42]. The full triangle at $Q^2 = 0$ is the RPP estimate [20]. The thick curves correspond to the results obtained in the LF relativistic quark models assuming that $N(1440)P_{11}$ is a first radial excitation of the $3q$ ground state: [15] (dashed), [19] (solid). The thin dashed curves are obtained assuming that $N(1440)P_{11}$ is a gluonic baryon excitation (q^3G hybrid state)